Intra-seasonal Variability (ISV) of Indian monsoon: Mechanisms, Predictability and Interaction with the mean

Lecture-10

B. N. Goswami
SERB Distinguished Fellow
Department of Physics, Cotton University, Guwahati

31 May, 2022

Schematic Representation Time scales associated with Weather and Climate Phenomena

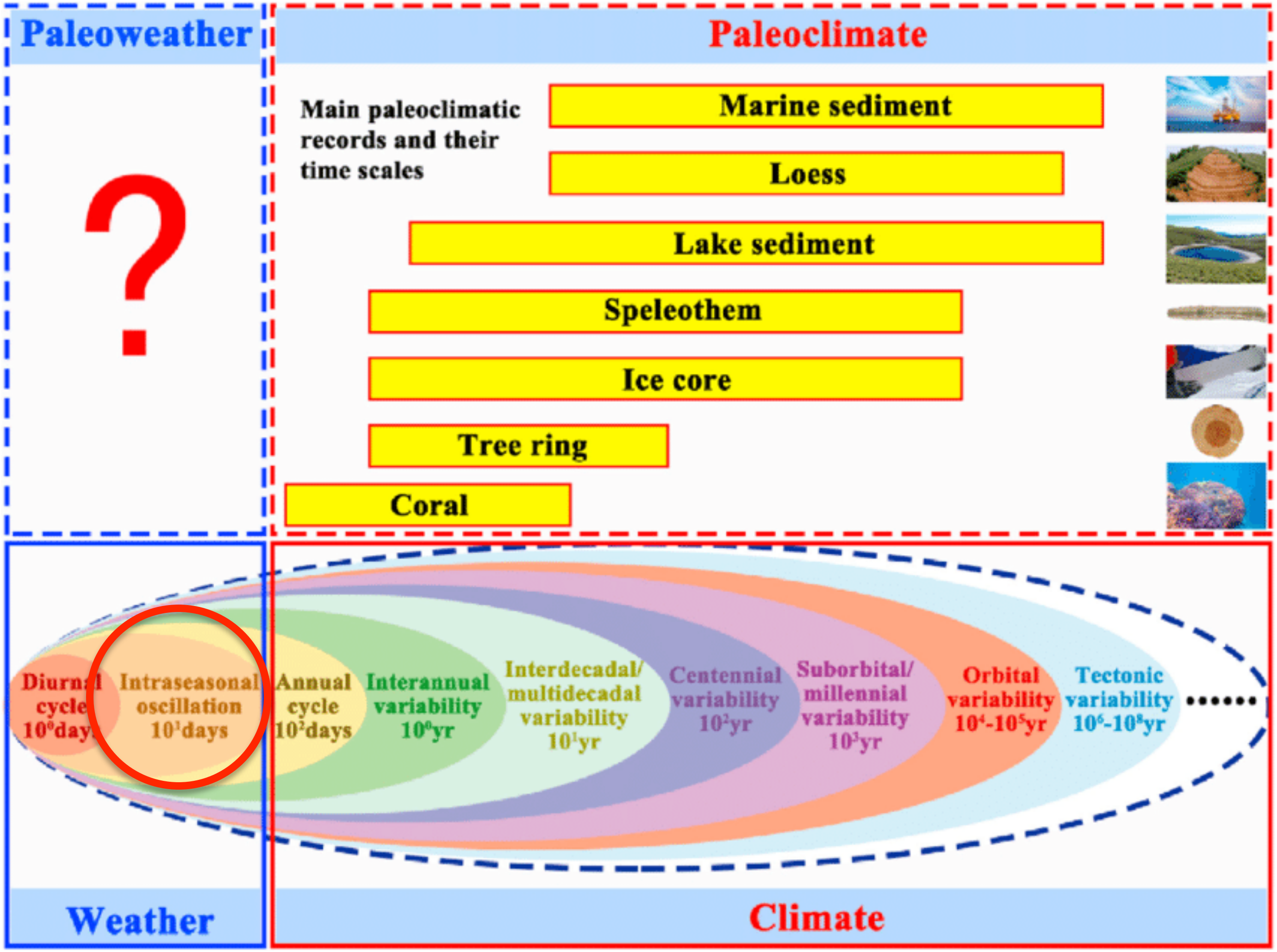

For a long time we thought All sub-seasonal variations are Weather. It changed in early 1970's when we discovered MJO and MISO that are distinctly different phenomena from those leading to Weather with 1-10 day time scales.

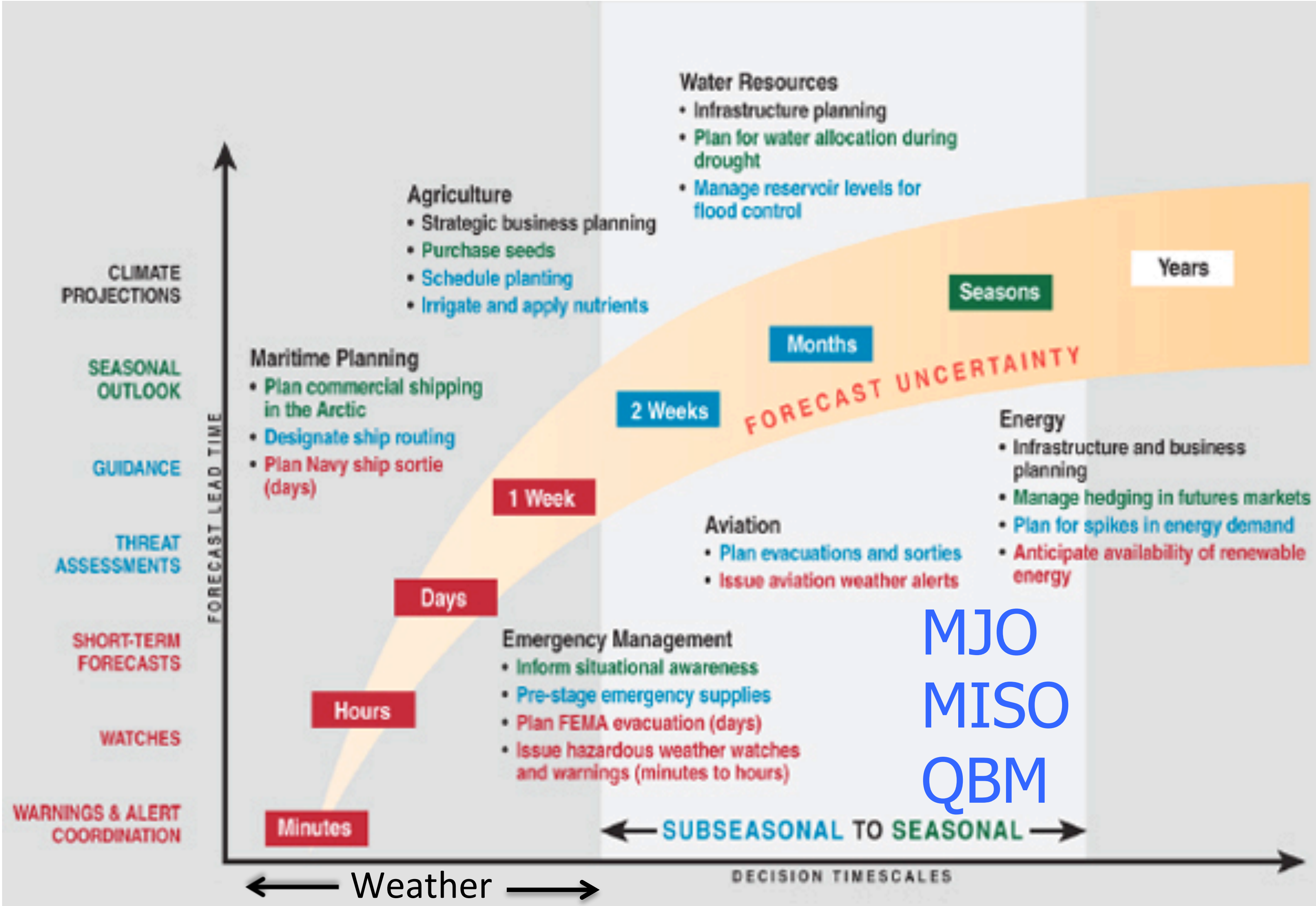

With that recognition, the time scales between 10-100 days is now known as Sub-seasonal to Seasonal **(S2S)** time scales, a bridge between Weather and Seasonal Climate. A new branch of research and prediction **(S2S)** has emerged

Here, we discuss Monsoon Intra-seasonal Oscillations (MISO and QBM), only other most important phenomena besides the MJO.

Outline

- Discovery of two dominant modes of ISV of Indian summer monsoon, namely
  - The 10-20 day mode, or the QBW mode
  - Boreal Summer or Monsoon ISO (MISO), 30-60 days
- Space-time characteristics of each Mode
  - Horizontal and Vertical scales
  - Propagation characteristics
- Scale selection
- Their influence on Indian Monsoon Weather & Climate

The Indian Summer Monsoon?

A manifestation of seasonal northward migration of the Rain Band or Tropical Convergence Zone (TCZ)

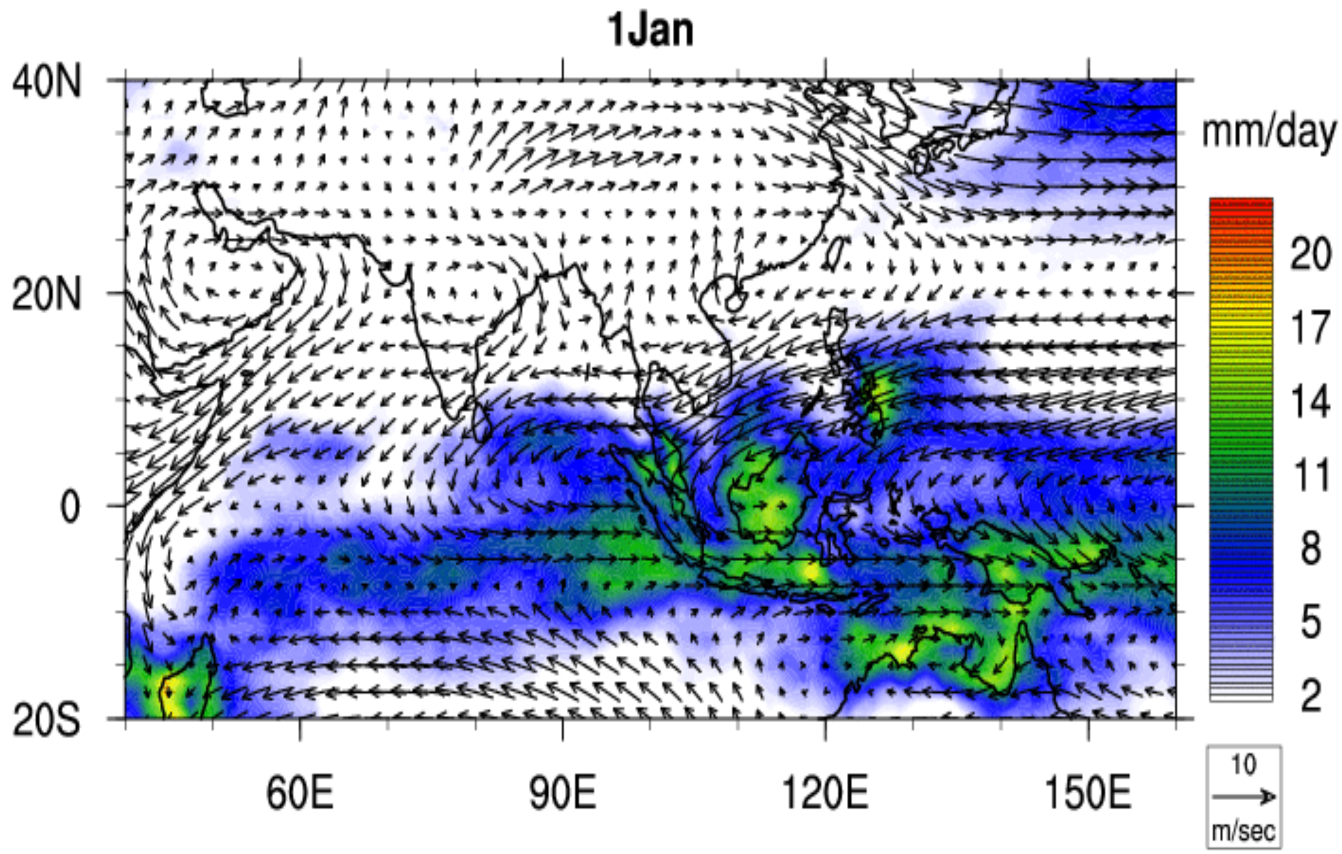

Annual evolution of Daily mean winds at 850 hPa and Precipitation (shaded)

Annual cycle of Precipitation over central India

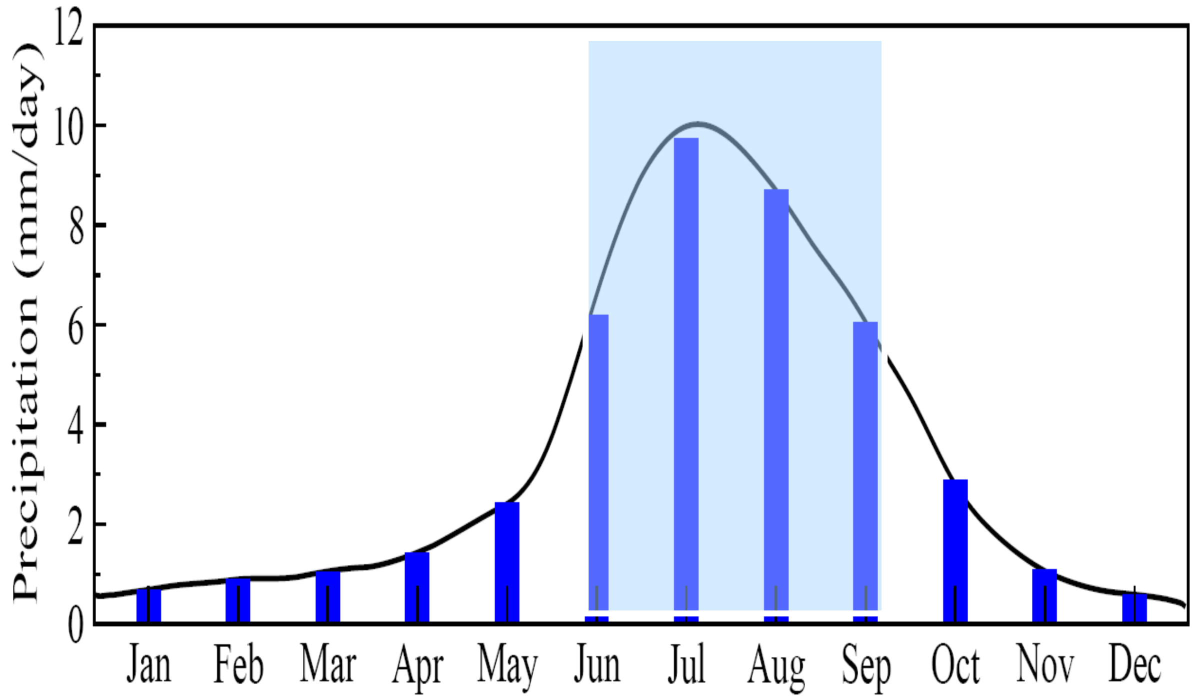

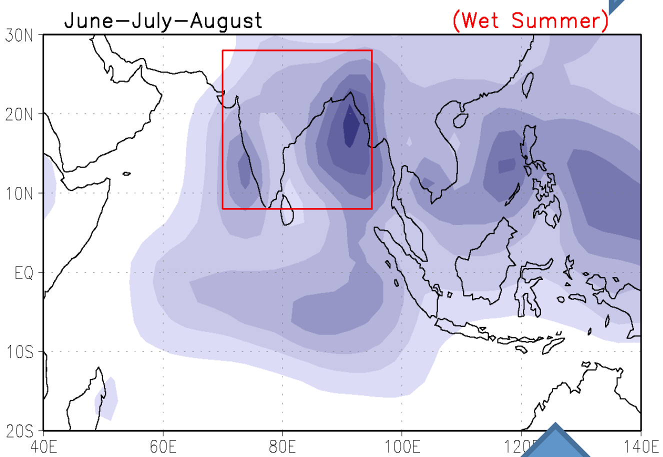

Seasonal mean JJAS precipitation

Daily Precipitation over India for two years

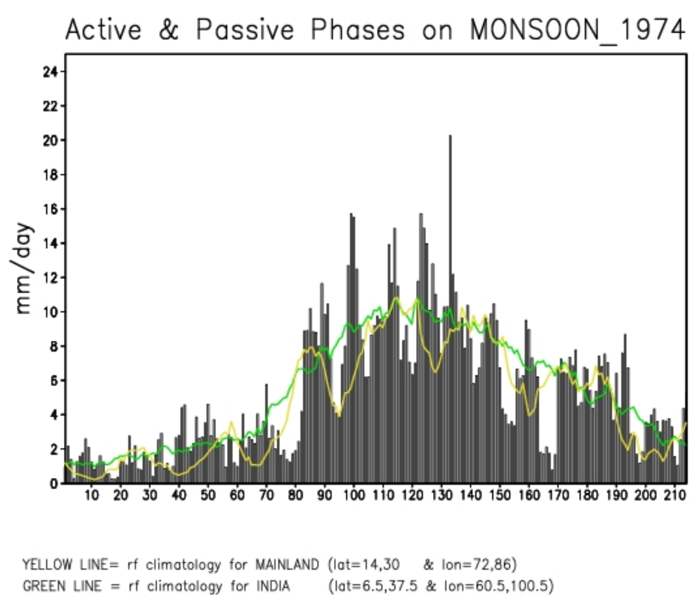

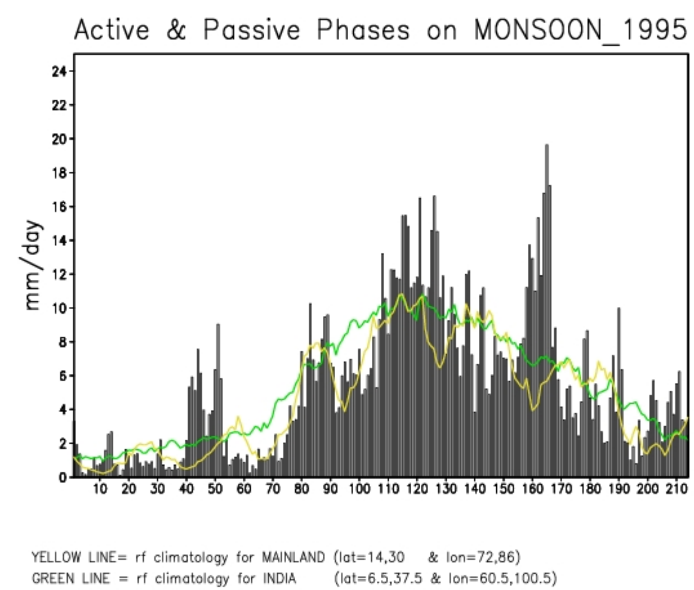

Indian Meteorologists were aware of sub-seasonal fluctuations in the form of

Active-break spells (cycles)

For a long time. e.g. Ramamurthy, 1962, 1969. However, large-scale characteristics were not well known.

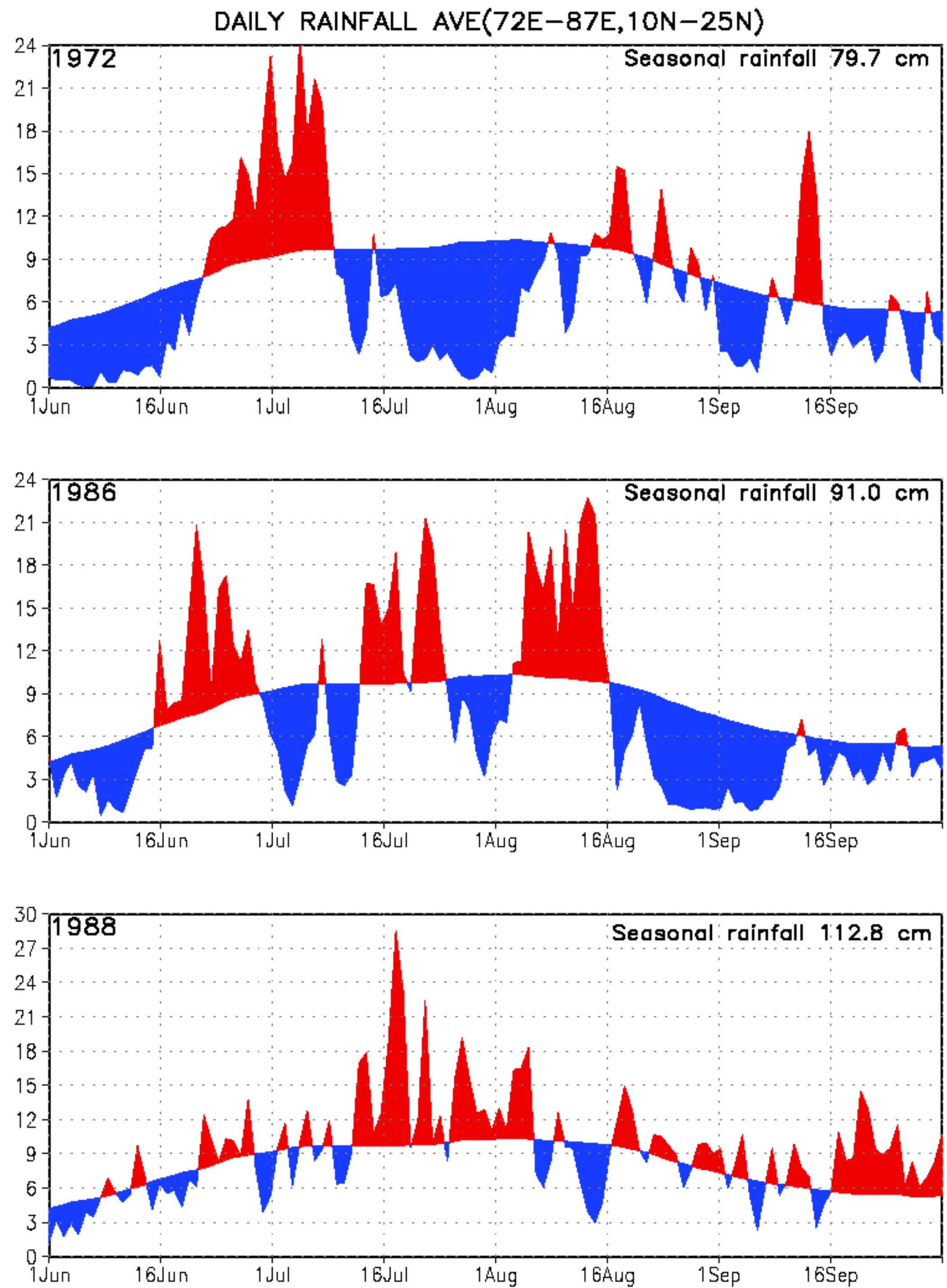

Daily rainfall (mm/day) over central India for three years, 1972, 1986 and 1988

The smooth curve shows long term mean.

Red shows above normal or wet spells while blue shows below normal or dry spells

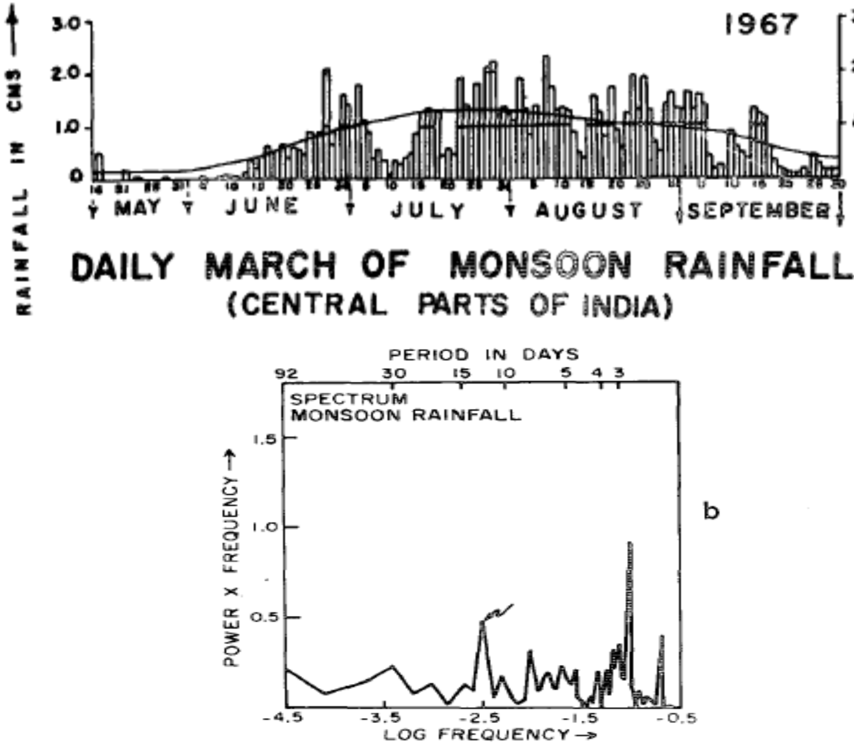

Fig. 15. Daily values of monsoon rainfall averaged over central India (a) and the power spectrum for monsoon rainfall (b).

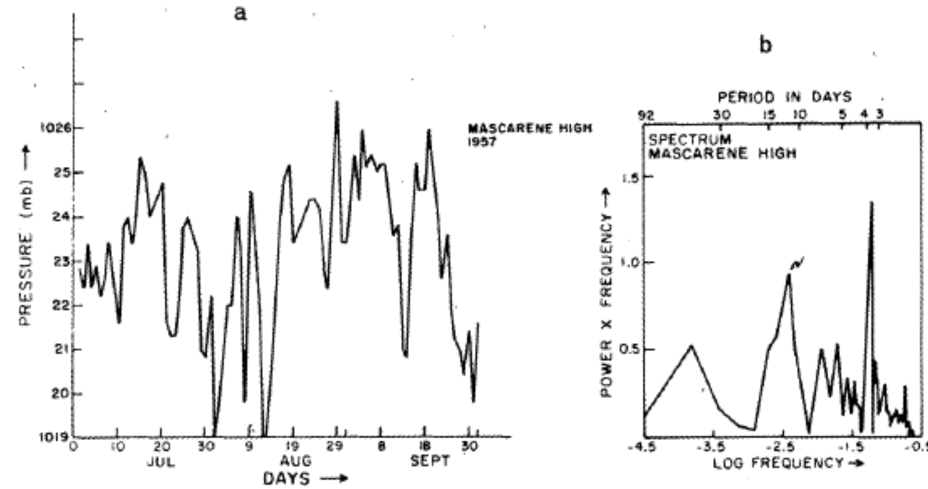

Fig. 10. As in Fig. 9 except over the Mascarene High.

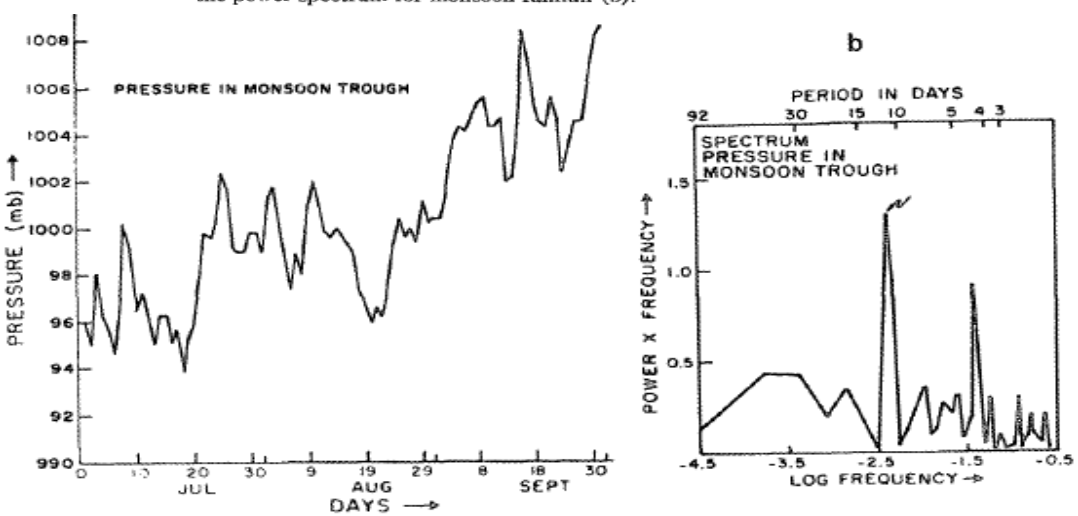

Fig. 9a. Daily mean sea level pressure over the monsoon trough. See Table 1 for the domain. The International Geophysical Year (IGY) data were used in this study. Fig. 9b. Power spectrum for the monsoon trough.

Krishnamurti and Bhalme 1976, JAS

Spectra of several time series related to Indian monsoon show a 10-20 day peak and a hint of a 30-60 day peak.

10-20 Day Mode or QBW

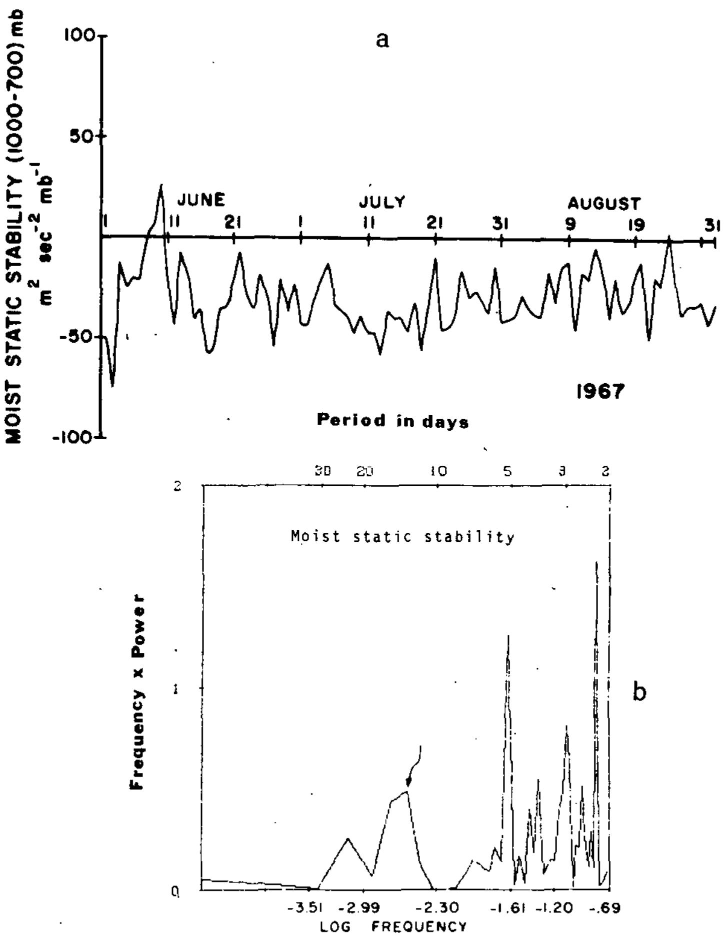

FIG. 17. As in Fig. 16 except for the moist static stability and the vertical layer 1000–700 mb.

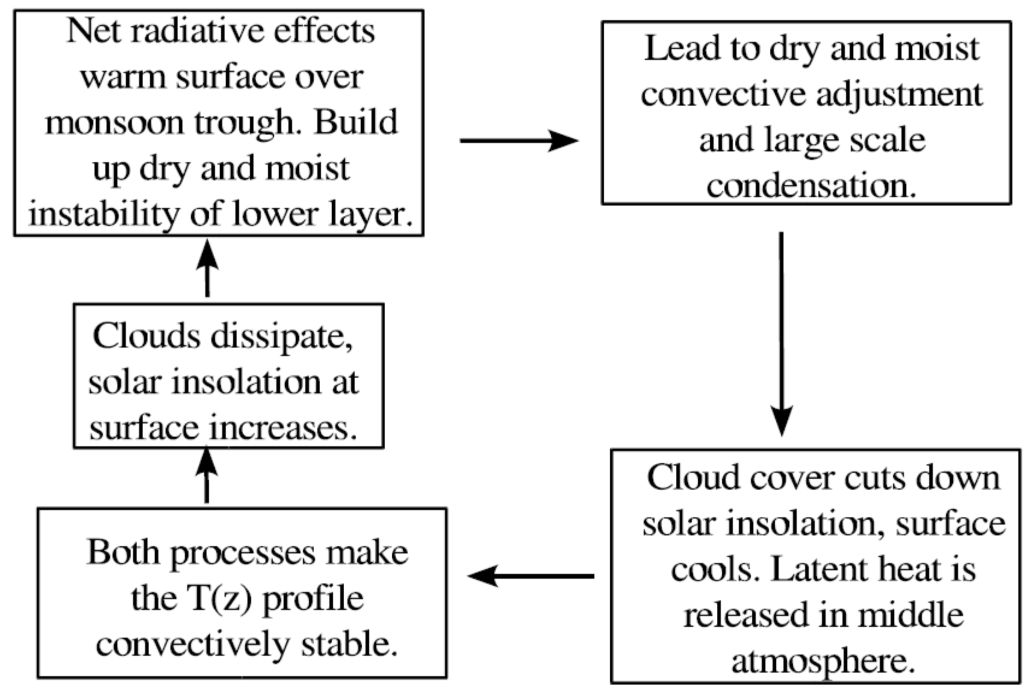

Figure 4: Schematic of the mechanism for 10-20 day mode proposed by Krishnamurti and Bhalme, 1976.

Moist static stability over central India shows 10-20 day oscillations

Krishnamurti and Bhalme, 1976, JAS

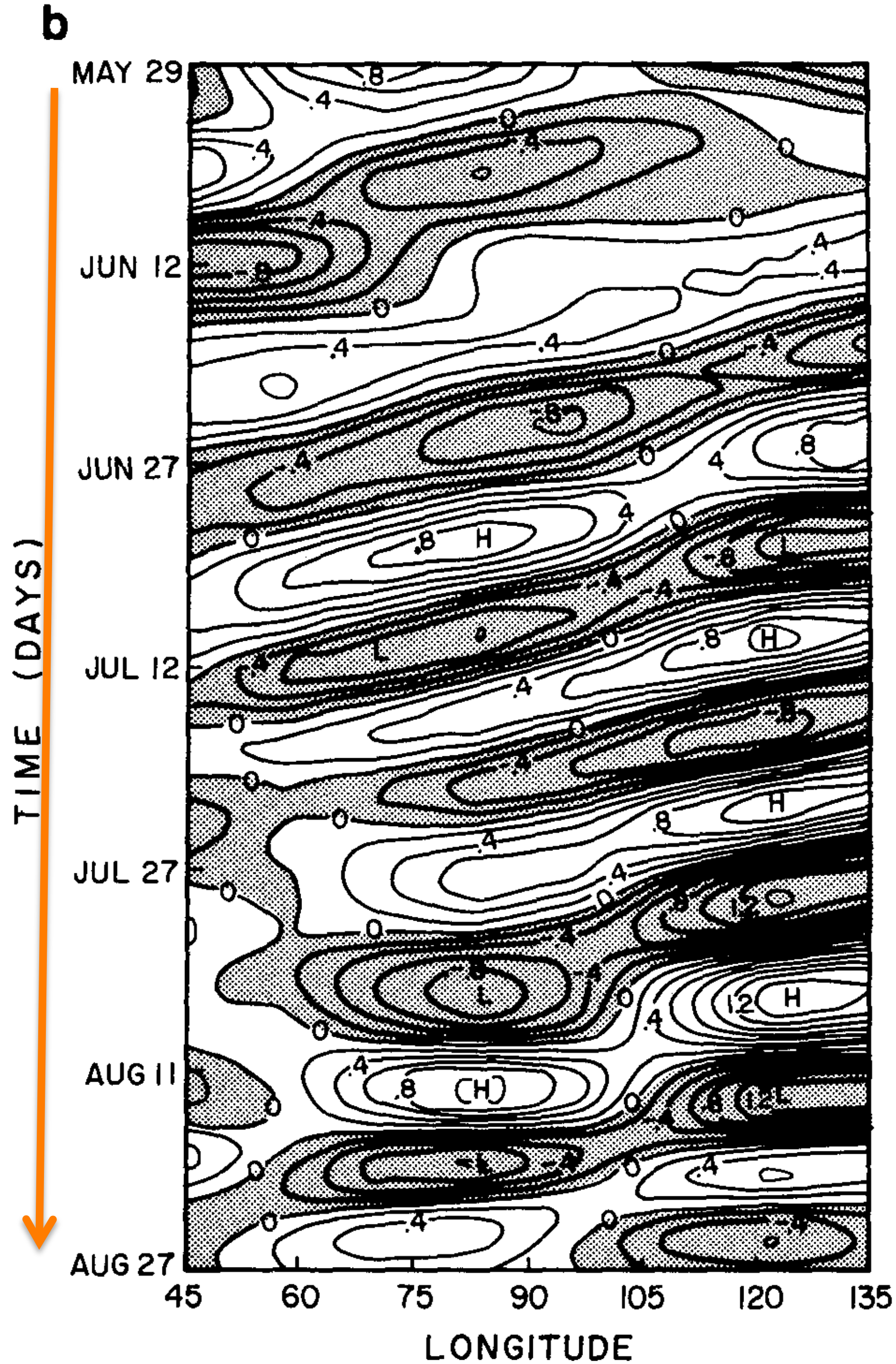

Some large-scale characteristics became clear when operational analysis became available

Krishnamurti, 1985, MWR (Based on FIGGE analysis for the year 1979)

Westward propagation of the 10-20 day wave from sea level pressure perturbation associated with the wave between 10N-20N.

Approximate phase speed ~ -7.0 m/s

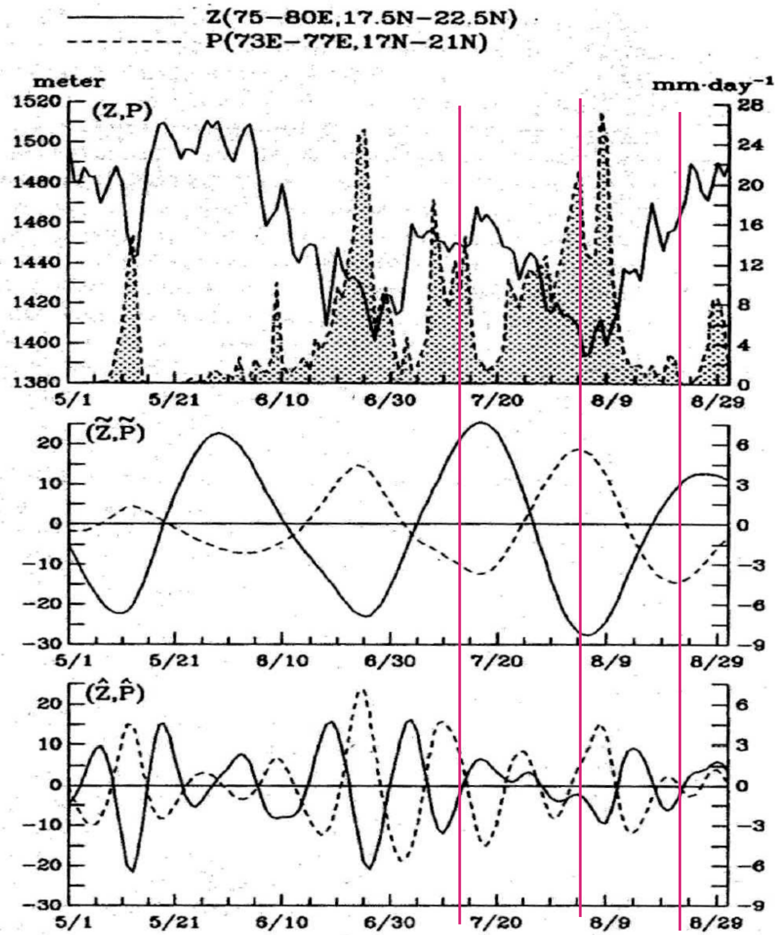

Figure 1.2: Fig (6) in [Chen and Chen, 1993] - The area averaged time series of precipitation P (dashed) over $(17^o - 21^oN, 73^o - 80^oE)$ and the 850 hPa height Z(850 hPa)(solid line) over $(17.5^o - 22^oN, 75^o - 80^oE)$ for year 1979: Top panel real time P (dashed) and Z(850 hPa) (solid), middle panel:30-60 day filtered $\tilde{P}$ (dashed) and $\tilde{Z}$(850hPa) (solid), and bottom panel: 10-20 day filtered precipitation $\hat{P}$ and $\hat{Z}$(850 hPa). The ordinates at the left and right sides of each panel represent height (m) and precipitation (mm day^{-1}), respectively. Dates of each time are denoted by month/day along abscissa.

Chen and Chen 1993, MWR

Used Indian monsoon rainfall for 1979 and FGEE IIIb data from ECMWF during summer

For the first time they showed that the 10-20 mode is associated with a Twin Cyclonic vortices centered around 10N.

Equatorial Rossby wave?

To bring out the robustness of characteristic features of the QBM and to examine the similarity in structure and propagation characteristics during summer and winter, we use

- **NCEP/NCAR reanalysis daily winds for 10 years (1992-2001)**
- **NOAA daily OLR for the same period**
- **GPCP daily precipitation**

→ **Examine spectra, for summer (1 June-30 Sept) and winter (1 Dec.-28 Feb. separately)**

→ **Filter data using a 10-20 day band pass Laczos filter**

→ **Define QBM index from the PC1 and PC2**

→ **Prepare phase composites**

Piyali Chatterjee and B. N. Goswami, 2004, QJRMS

CEOF of 10-20 day filtered zonal and meridional winds at 850 hPa and OLR between June 1 and Sept.30 for 10 years, 1992-2001.

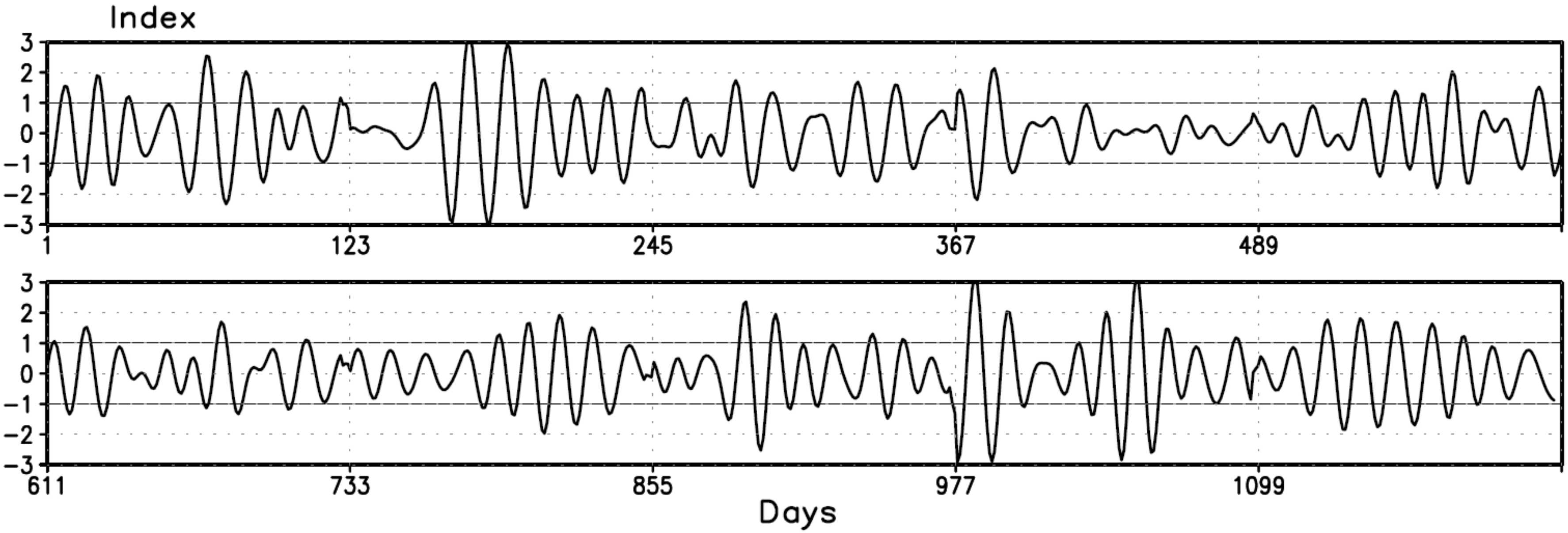

Figure 2. Quasi-biweekly mode index derived from the first two principal components of the combined empirical orthogonal function of 10–20 day filtered zonal and meridional winds at 850 hPa and outgoing long-wave radiation for 10 years, normalized by its own standard deviation.

QBM Index : {PC1(t) +PC2(t-4)}/2

Take all events having normalized amp. > 1. Create phase composites for all 15 phases from phase 1 (peak) to phase 8 (trough) to phase 15 (next peak) .

Summer composite

850 hPa 10-20 day filtered winds and OLR for two opposite phases (a,b) of the QBM . (c) Relative vorticity (x 1.0e+6) averaged between 5S-5N as a function 15 phases

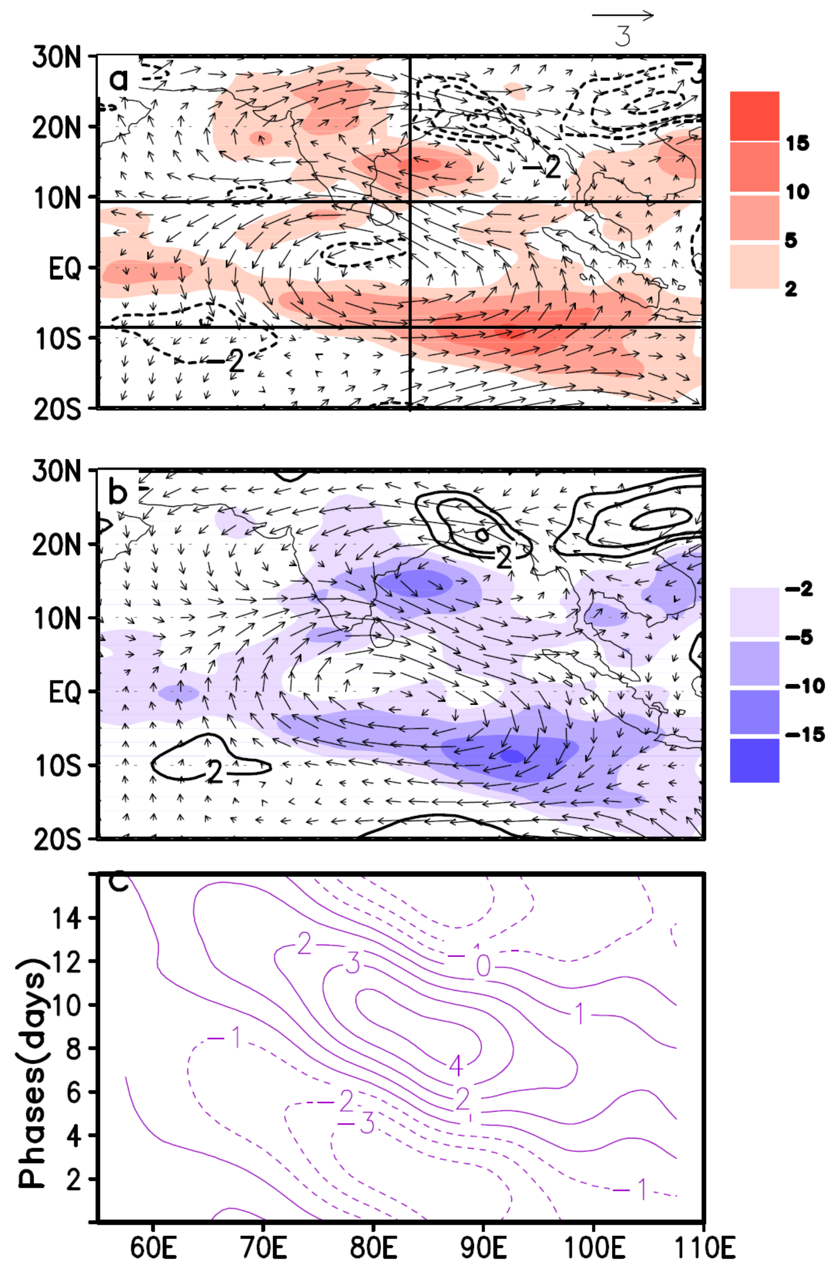

$C_p \sim 4.5$ m/s

$\lambda \sim 6000$ km

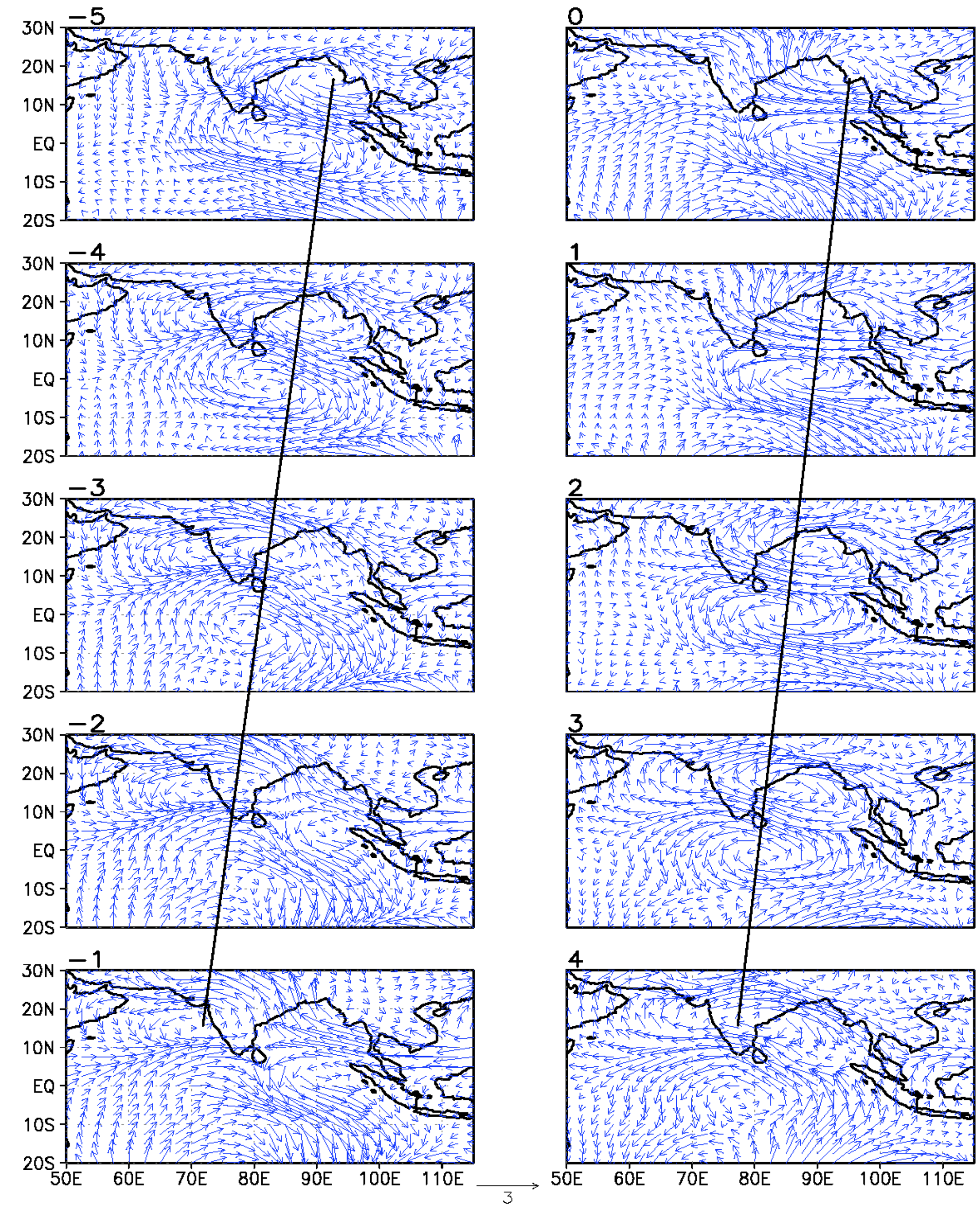

Figure 5: Composites of different phases showing generation and westward movement of vortices. The scale for wind vectors is same for all levels and shown at the bottom.

Composite structure for different phases.

Westward phase propagation of the two vortices is evident

Winter composite

850 hPa 10-20 day filtered winds and OLR for two opposite phases (a,b) of the QBM . (c) Relative vorticity (x 1.0e+6) averaged between 5S-5N as a function 15 phases

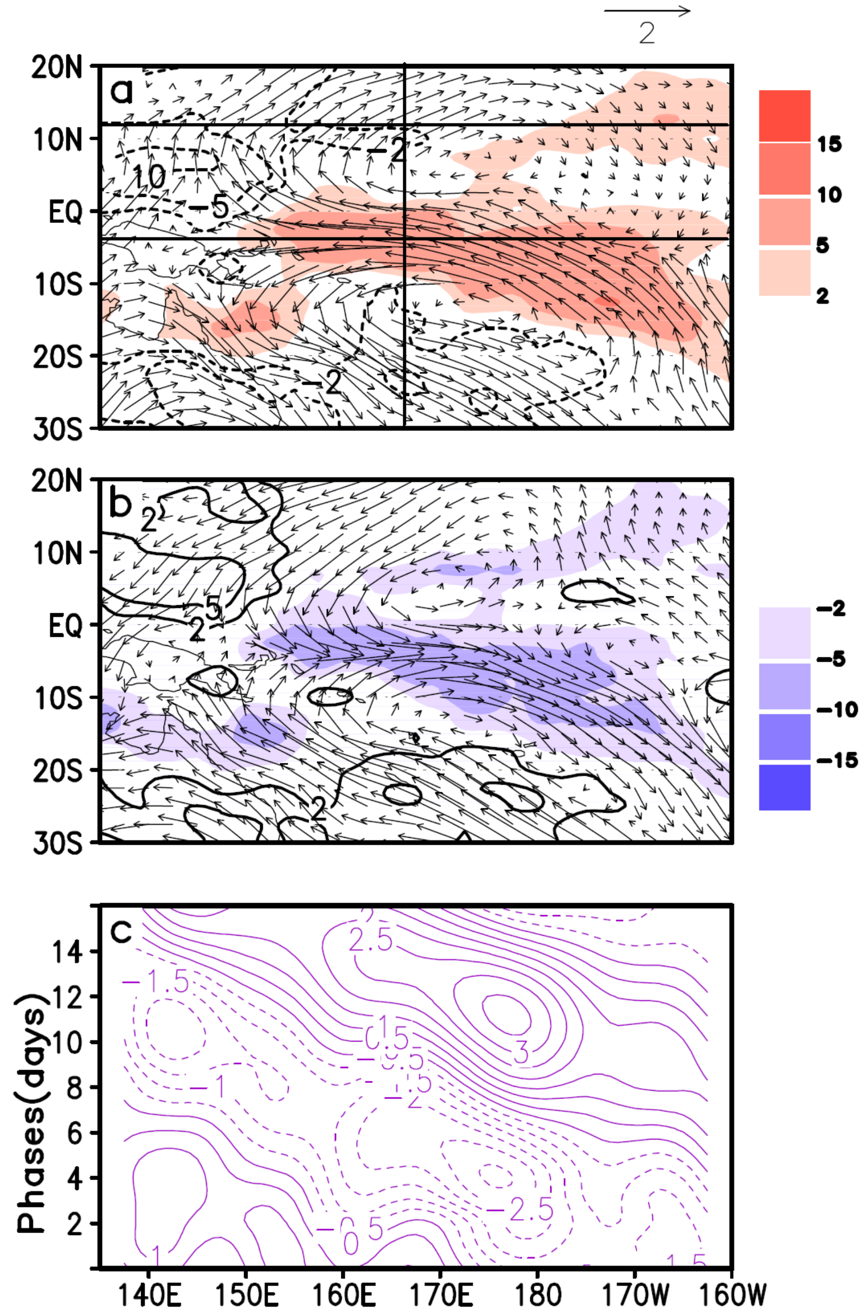

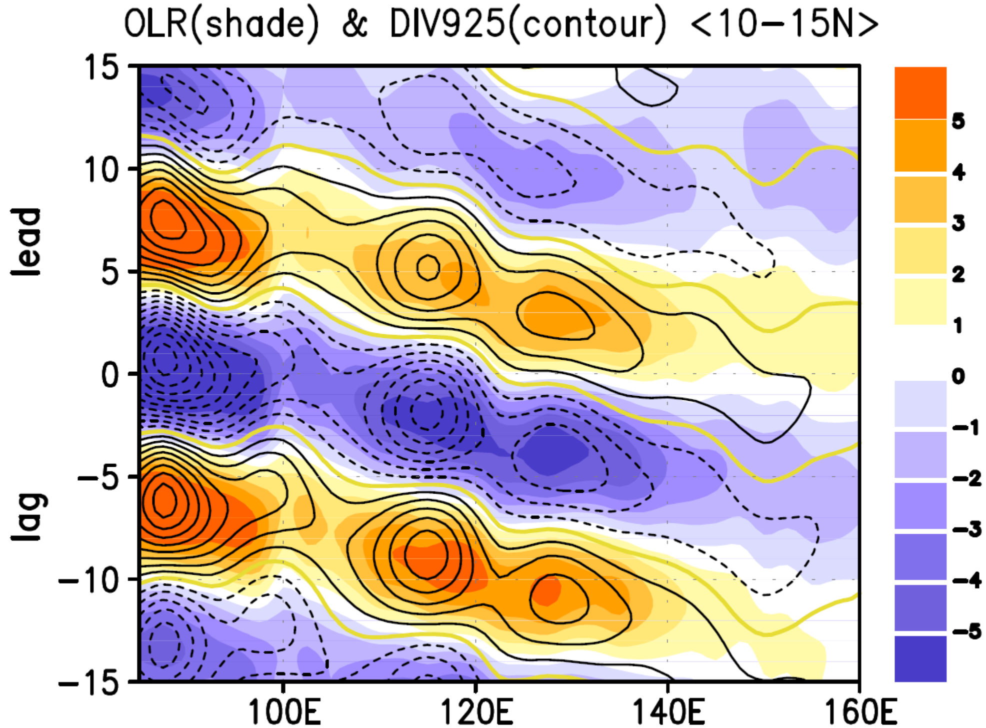

Lag-longitude plot of Regression of 10-20 day filtered OLR and 925 hPa div. on the QBM index averaged between 10N-15N.

Div. Maximum (minimum) at 925 hPa (BL) is west of the OLR maximum (minimum).

➔BL moisture convergence makes convection move westward

➔Convective coupling

Chatterjee and Goswami, 2004, QJRMS

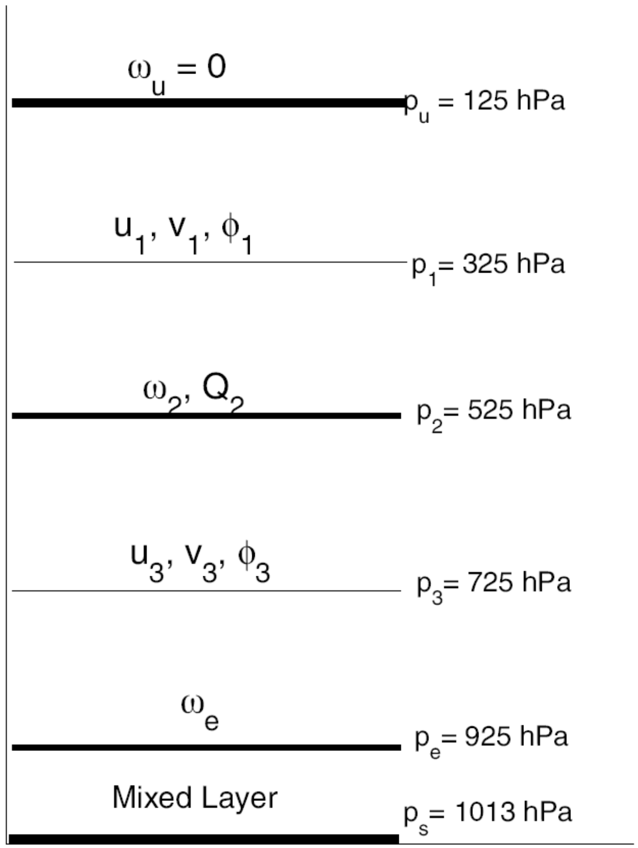

Figure 6. The vertical structure of the model.

Momentum eqns.at levels 1 and 3 while the thermodynamic energy eqn.at level 2.

Define barotropic and baroclinic components as

$$\chi_{\mathrm{c}} = (\chi_3 - \chi_1)/2 \text{ and } \chi_{\mathrm{t}} = (\chi_3 + \chi_1)/2,$$

Where χ represents zonal and meridional winds u and v or geopotential Φ, Ū represents mean background flow.

$$Q_2 = bgL_{\mathrm{w}}P/\Delta p.$$

$$Q_2 = -\frac{bL_{\mathrm{w}}}{\Delta p}[\omega_2(\overline{q}_3 - \overline{q}_1) + \omega_{\mathrm{e}}(\overline{q}_{\mathrm{e}} - \overline{q}_3)] + \mu\frac{2C_p p_2}{R_{\mathrm{gas}}\Delta p}\phi_{\mathrm{c}} + \Lambda^* u_{\mathrm{B}}$$

Results: The control case; No mean flow, No EWF

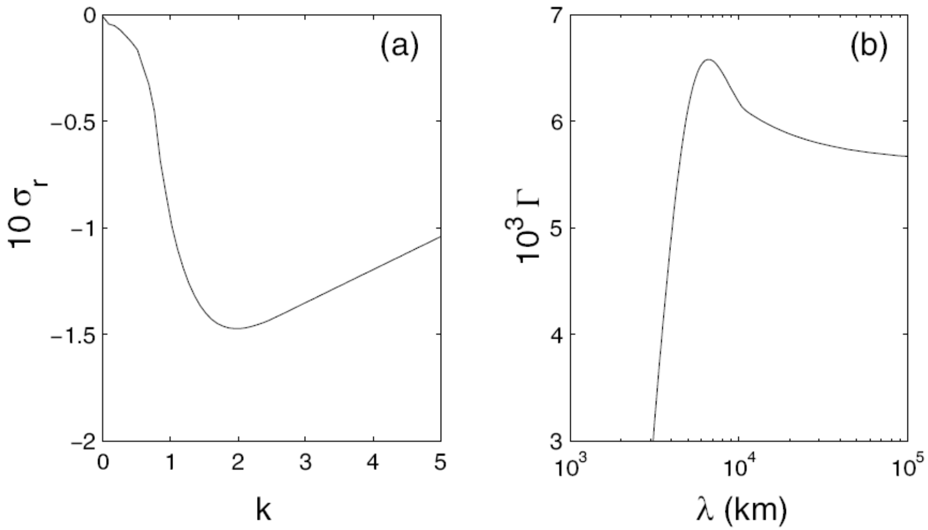

(a) Wavenumber vs real freq.

(b) Growth rate Γ vs wave length

Max Growth for k=1.33, or λ=6750 km.
Period=16 days, Cp= 4.8 m/s

Structure of the most unstable , n = 1 Rossby mode

Vortices symmetric about the equator

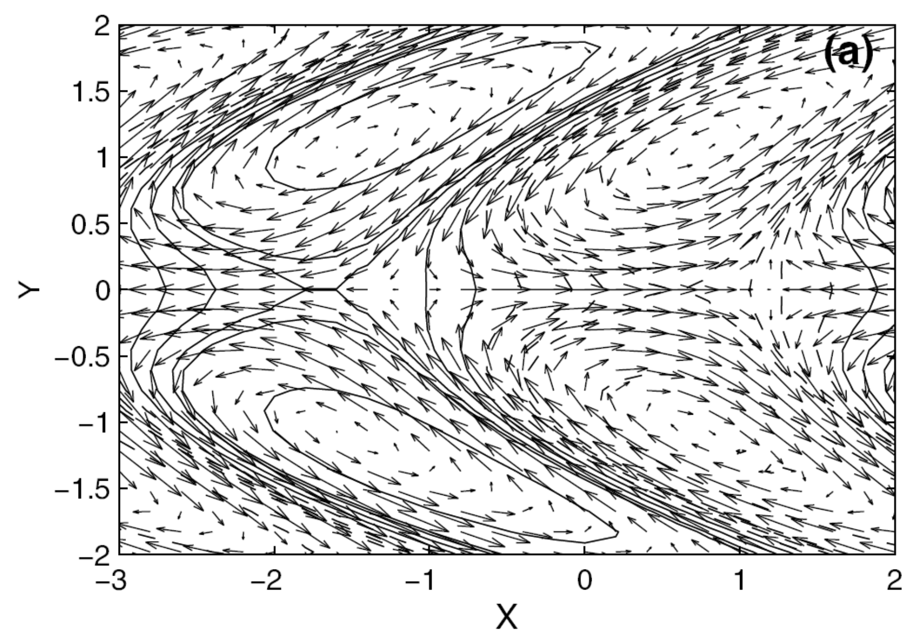

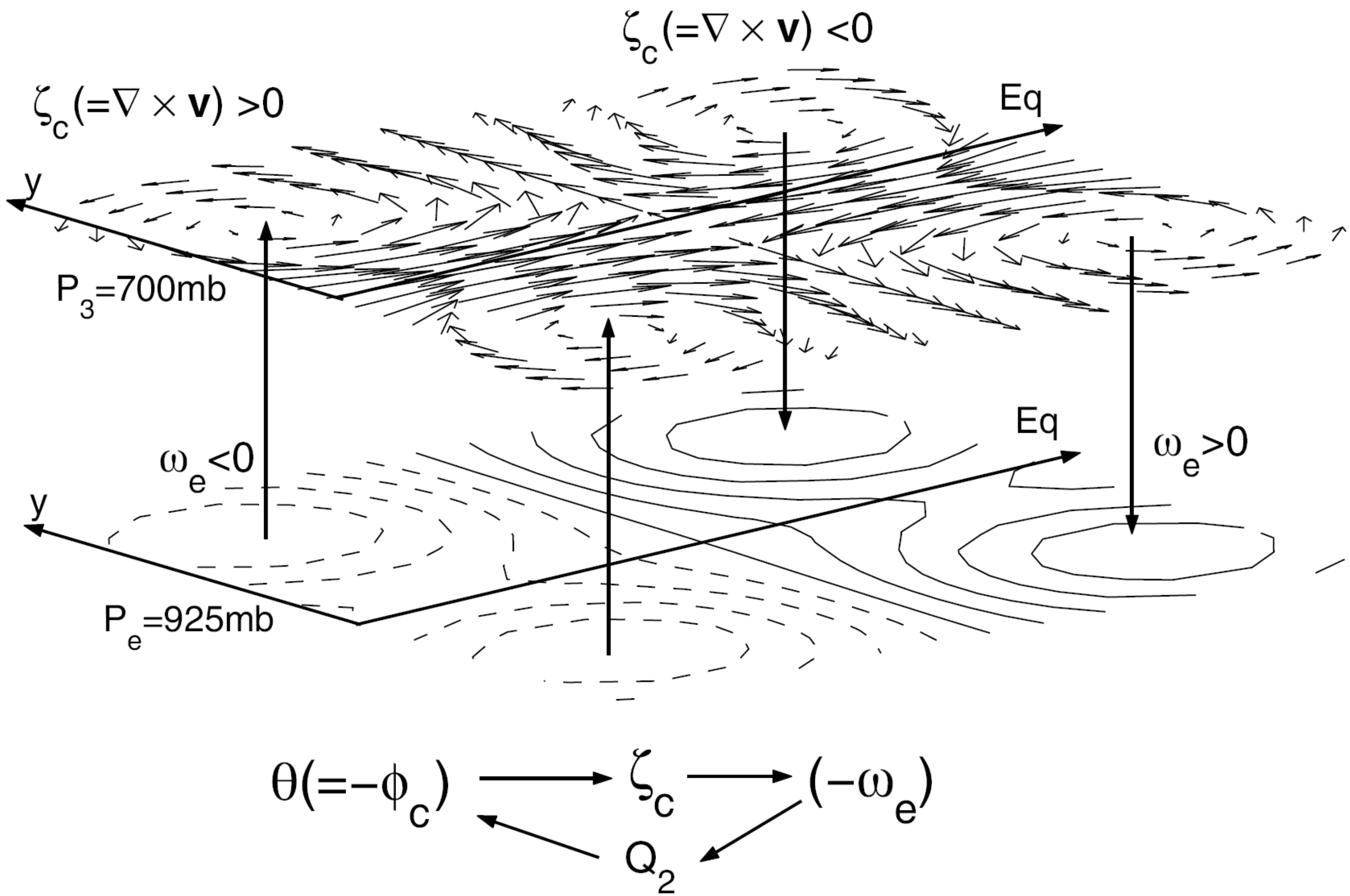

Schematic illustrating the Wave-Boundary-Layer-CISK for the unstable mode

There is a clear quasi-biweekly oscillation in equatorial Indian Ocean

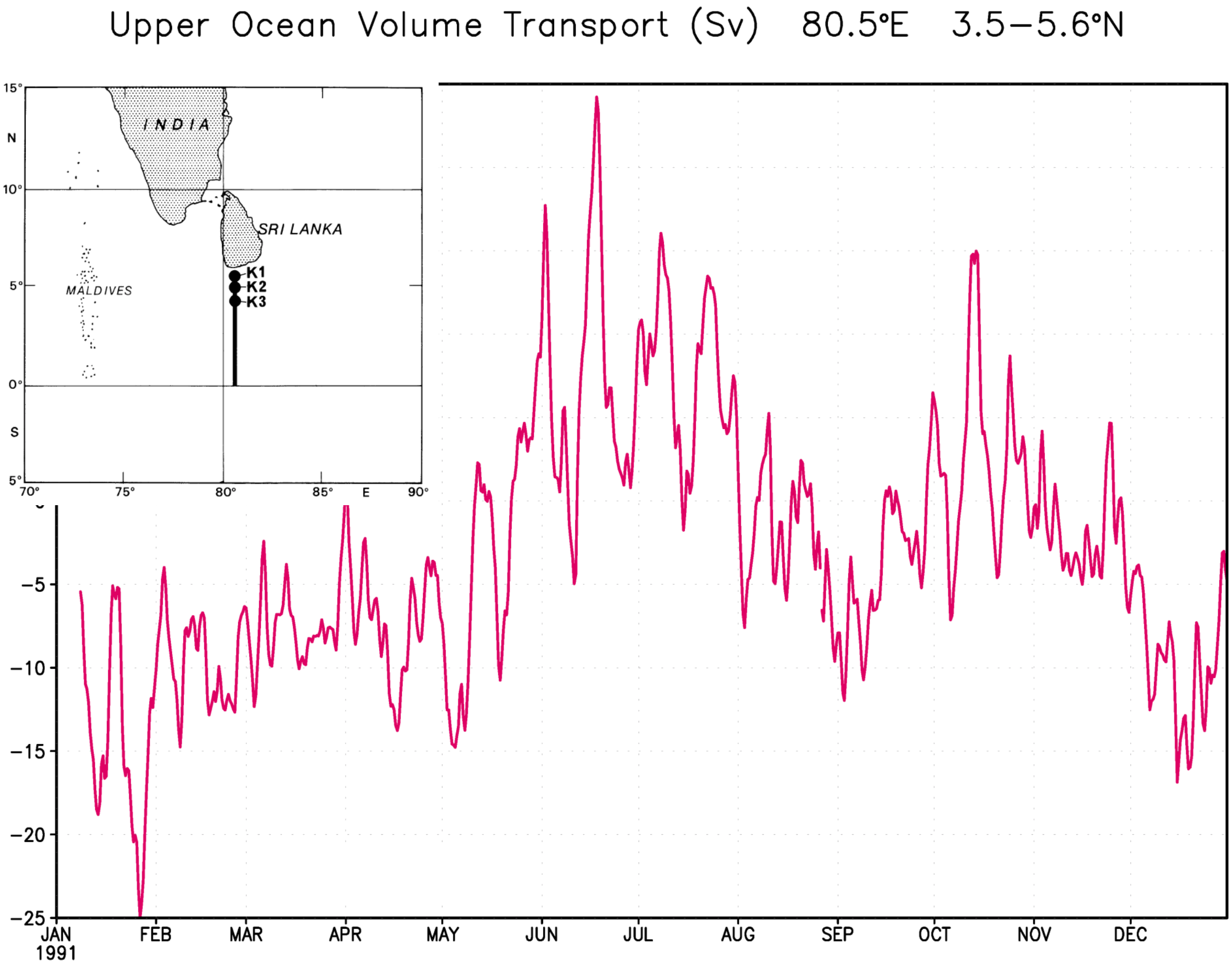

Schott et al., 1994, JGR

MERIDIONAL VELOCITY (cm s^{-1}) 90°E EQUATOR

OBSERVATION *(Masumoto, Murty et al., Presented at IOGOSS Conference, Mauritius, November 2002)*

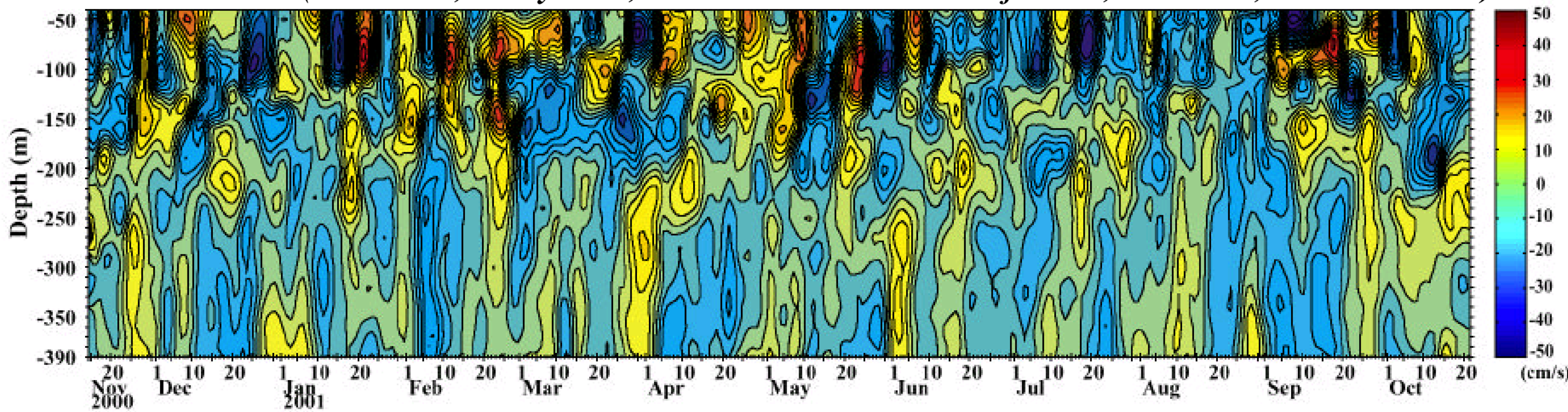

From Sengupta et al, 2007, J. Climate

MODEL

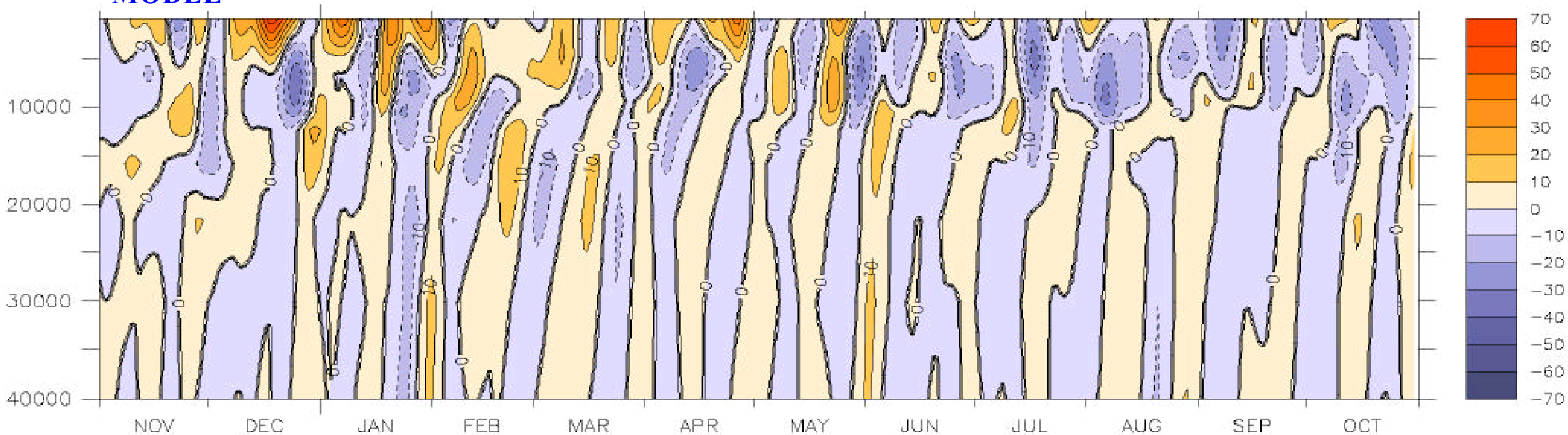

The 30-60 day mode or the Monsoon Intraseasonal Oscillation (MISO)

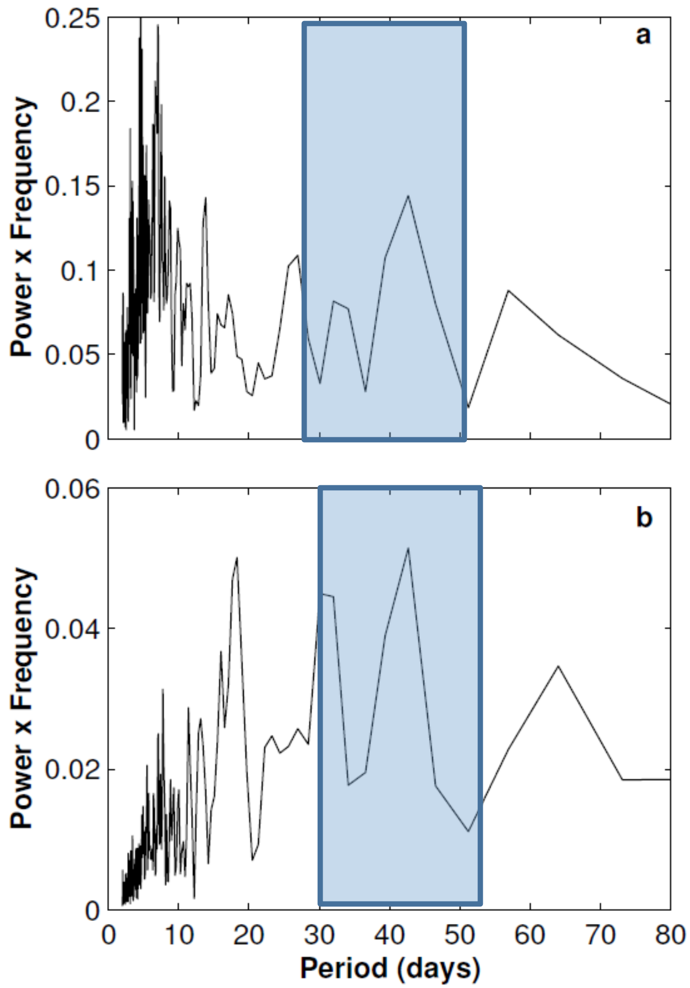

Figure 1: Spectrum of (a) rainfall anomalies for 20 (1971-1989) summer seasons (1 June -30 September) from station data averaged over 75E-85E and 15N-25N and (b) zonal wind anomalies at 850 hPa for 20 (1979-1998) summer seasons from NCEP reanalysis averaged over 55E-65E and 5N-15N.

Existence of sub-seasonal oscillations in the time-scale of about a month has been known to Indian meteorologists for a long time (e.g. Dakshinamurthy and Keshavamurthy, 1976) .

However, their spatial scale and propagation characteristics became clear only after 1979.

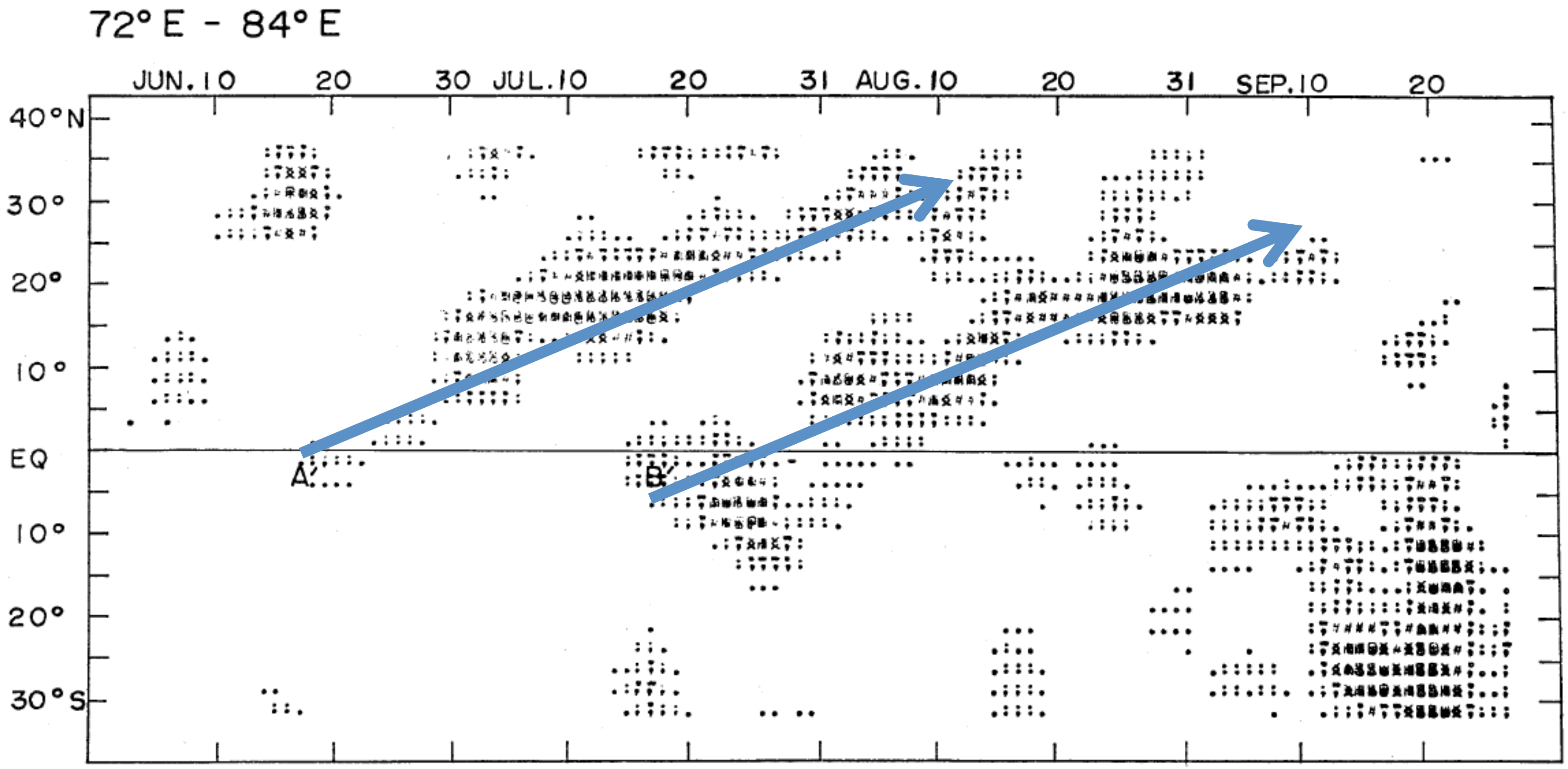

Fig. 7 Time-latitude sections of cloudiness for 72°–84°E longitude zone. Time means are subtracted from the smoothed cloudiness, and positive deviations are illustrated by the grey scale. The cloudiness difference between adjacent levels is 0.3. See text for the symbols A′ and B′.

Yasunari, 1979, JMSJ

For the first time the cloud bands were shown to propagate regularly northward with a period of over a month

Northward Propagation of Maximum Cloud Zones
Sikka and Gadgil, MWR (1980)

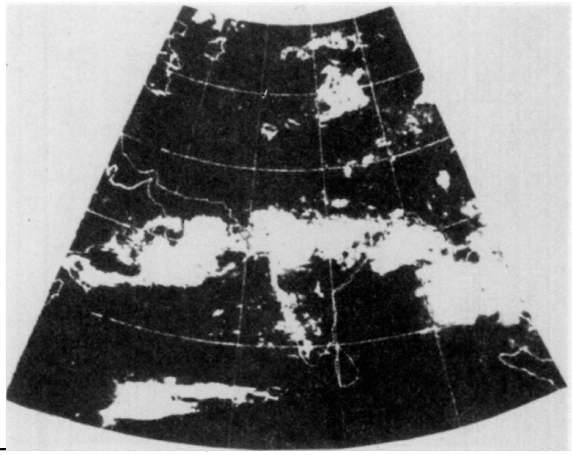

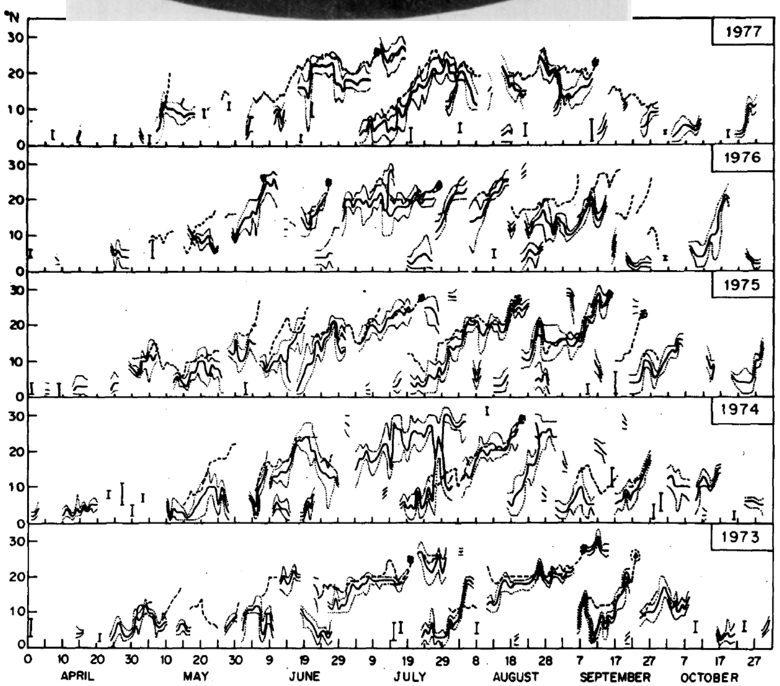

Fig. 4. Daily variation of the latitude of the axis of the MCZ (solid line); northern and southern limits (dotted line) of the MCZ; and the location of the 700 mb trough (dashed line) at 90°E during 1973–77.

- **Two favorable locations for maximum cloud zones (tropical Convergence Zones, TCZs) are identified; one over the equatorial Indian Ocean and other over Monsoon zone north of 15°N.**
- **Revival of the monsoon occurs with a transition to a moist convective regime, either with northward propagation of the equatorial TCZ**
- **Established large scale nature and propagation characteristics of Monsoon ISOs**

Almost simultaneously, Sikka and Gadgil showed similar northward propagation of the cloud bands.

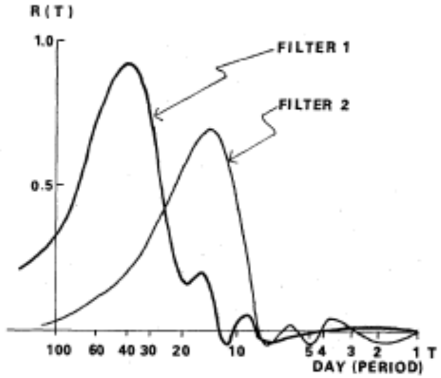

Fig. 4 Frequency response of the two filters. The peak of filter 1 exists at 40-day period and that of filter 2 is at about 14-day period.

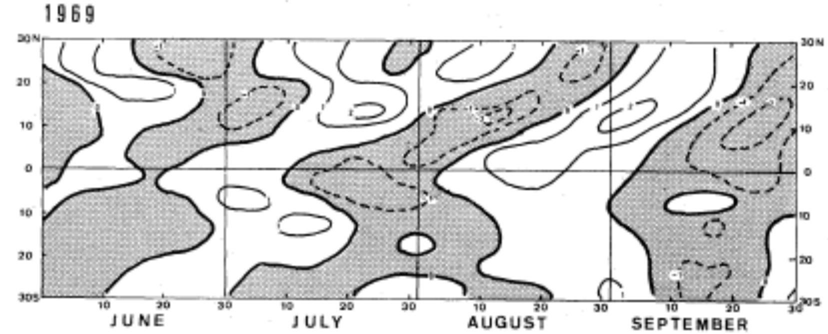

Fig. 3 Time latitude section of filtered cloudiness for the 40-day period along the longitudinal sector of 70°-90°E. Unit of contour line is 1.0 and negative values are shaded.

Yasunari, 1981, JMSJ

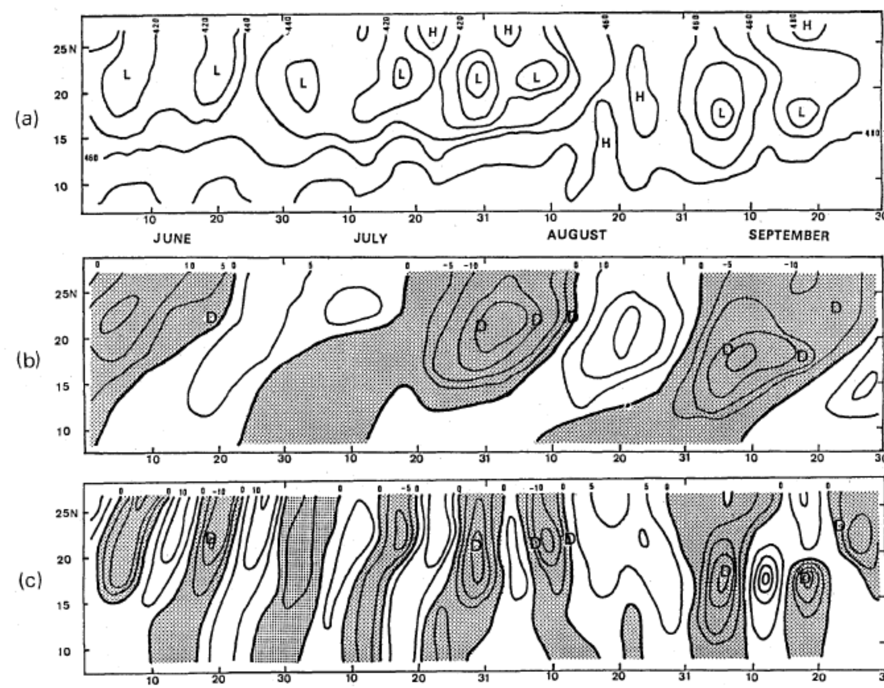

5 Cross sections of the geopotential height at 850 mb along the line shown in Fig. 1, by using (a) 5-day moving averaged data (b) data by filter 1, and (c) data by filter 2. Contour intervals are (a) 20 m, (b), (c) 5 m. The areas of negative values are shaded in (b) and (c).

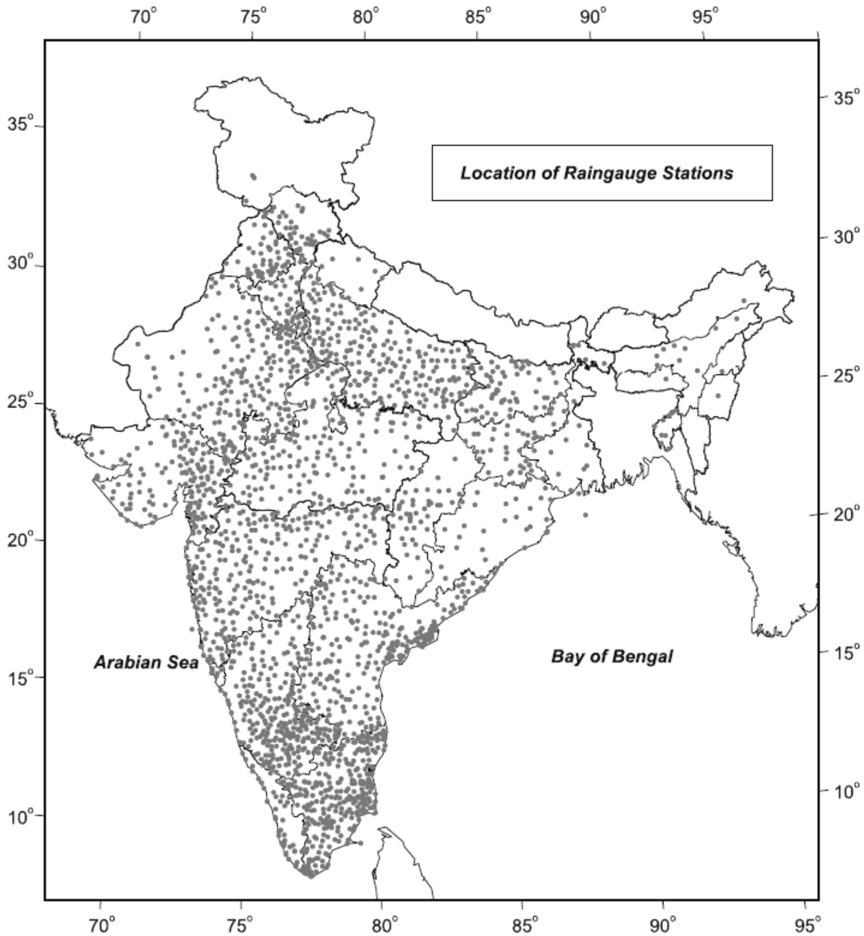

Figure 3. Network of raingauge stations considered for the development of high resolution gridded dataset.

Rajeevan,Gadgil and Bhate, 2010, JESS,

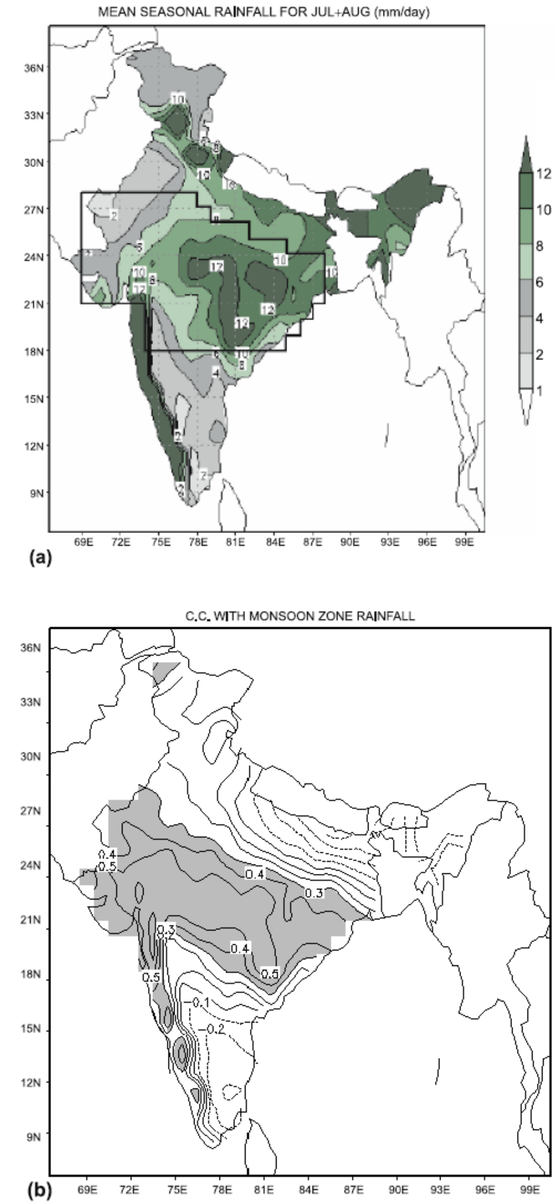

Figure 4. (a) Monsoon core zone considered to identify the active and break events. Mean (1951–2007) rainfall (mm/day) during the period July and August is also shown. (b) Correlation coefficient of 5-day average rainfall over the monsoon zone with rainfall at all grid points. Rainfall during only July and August months have been considered.

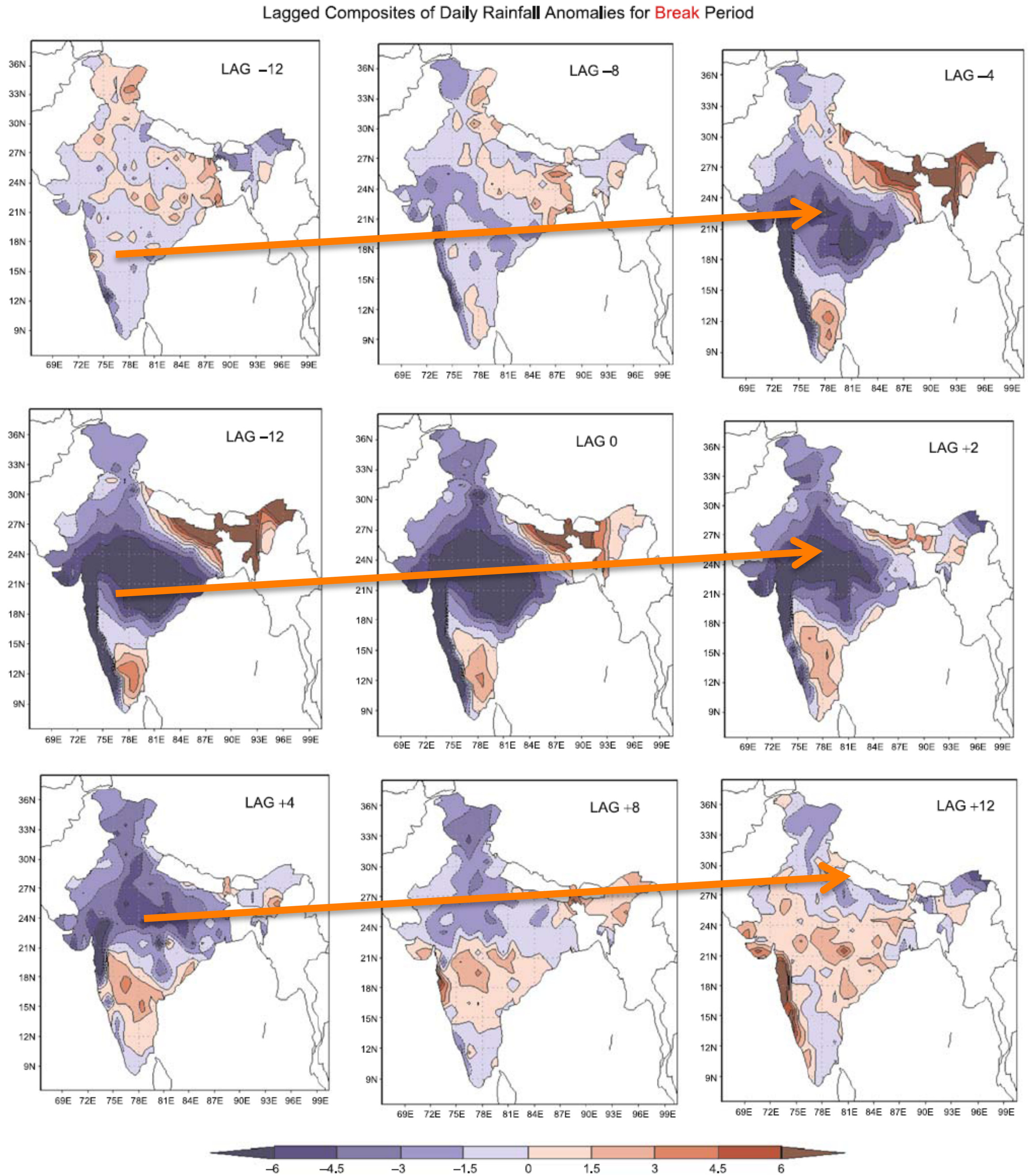

Figure 7(a). Lagged rainfall (mm) composites during the break spells (1951–2004).

Break Composite

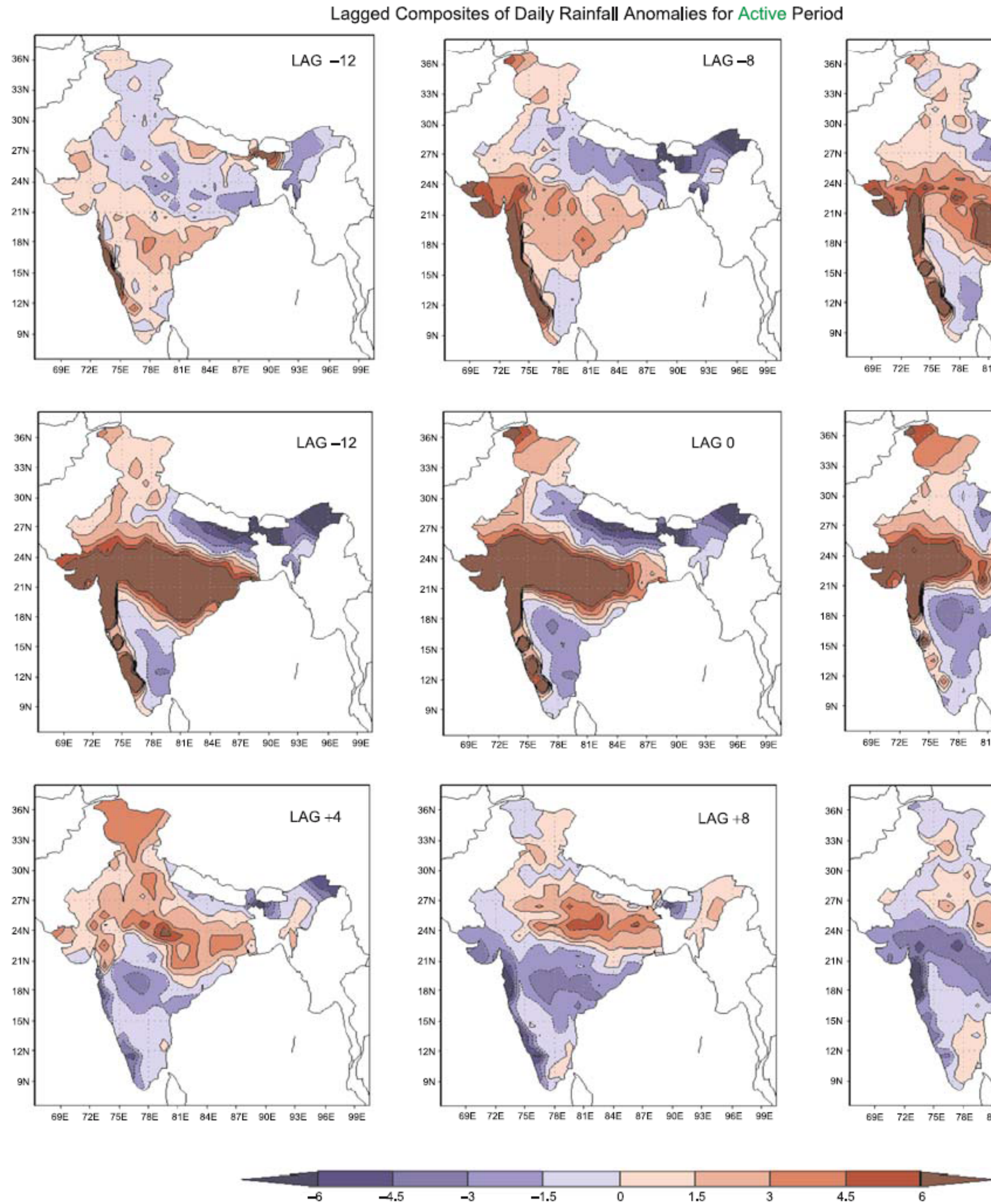

Figure 7(b). Lagged rainfall (mm) composites for the active spells (1951–2004).

Active Composite

MISO is not confined only within India and has a large scale spatial structure

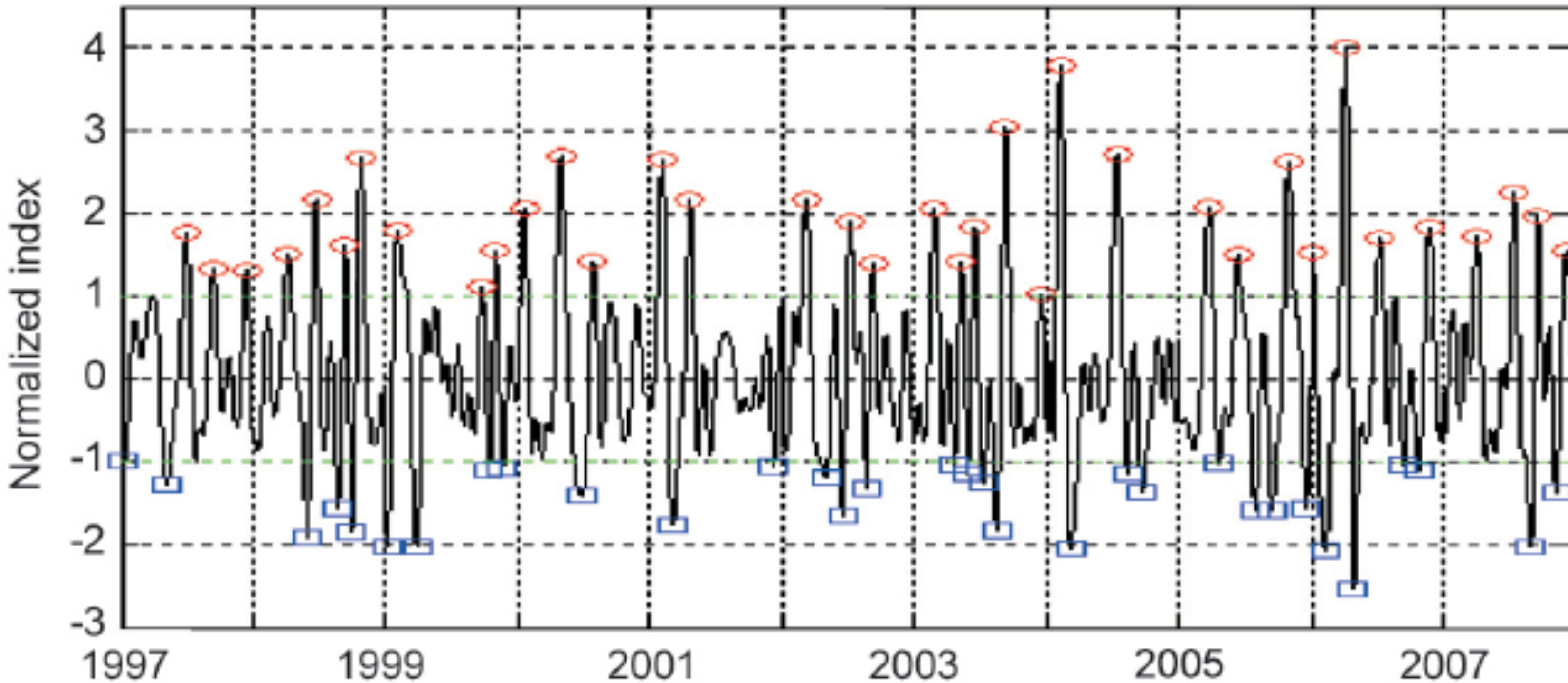

Figure 2.4. Time series of normalized monsoon ISO index between June 1 and September 30 (122 days) for a sample of 11 (1997–2007) summer seasons. The ISO index is defined as 10 to 90-day filtered GPCP rainfall anomaly averaged between 70°E–90°E and 15°N–25°N. The time series is normalized by its own standard deviation. Open circles and squares indicate peaks of active and break conditions, respectively.

Lag composite of MISO: 25-90 day (GPCP JJAS)

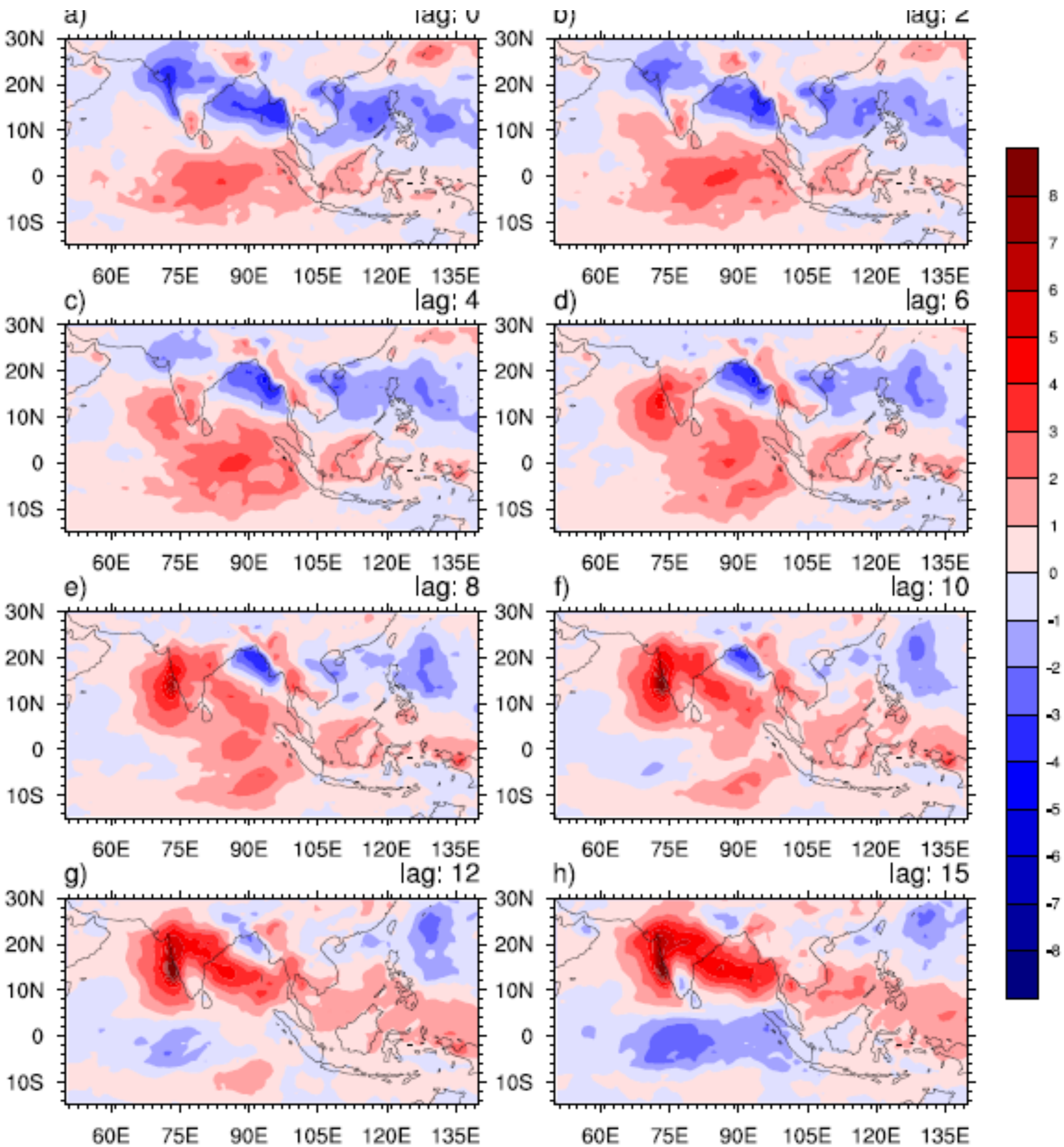

MISO evolution one half cycle

- Large east-west scale
- Meridional dipole Over Indian region
- NW-SE tilt of the rainband

Suhas,Neena,Goswami, 2014, Climate Dynamics

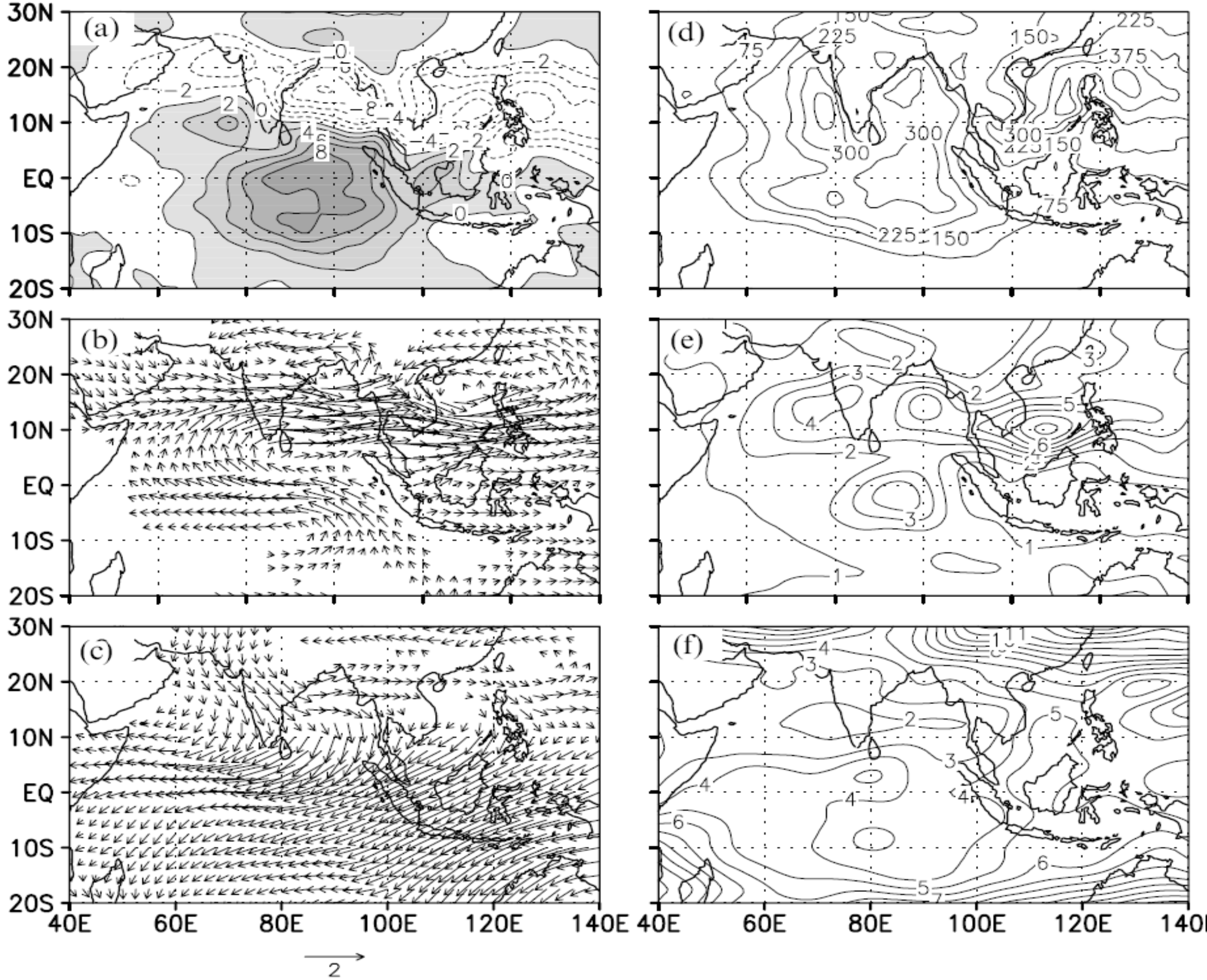

Figure 2.10. Spatial structure and amplitude of the 30–60-day mode. Regressed 30–60-day filtered anomalies of (a) OLR (in $\mathrm{W\,m^{-2}}$), (b) 850-hPa winds, and (c) 200-hPa winds (in $\mathrm{m\,s^{-1}}$) with respect to a reference time series of 30–60-day filtered zonal winds averaged over 85°E–90°E and 5°N–10°N with 0 lag. Only regressed wind anomalies significant at 95% confidence level are plotted, with a mean variance of 30–60-day filtered (d) OLR (in $\mathrm{W^2\,m^{-4}}$), (e) 850-hPa, and (f) 200-hPa zonal winds (in $\mathrm{m^2\,s^{-2}}$), based on 20 (1979–1998) summers (1 June–30 September).

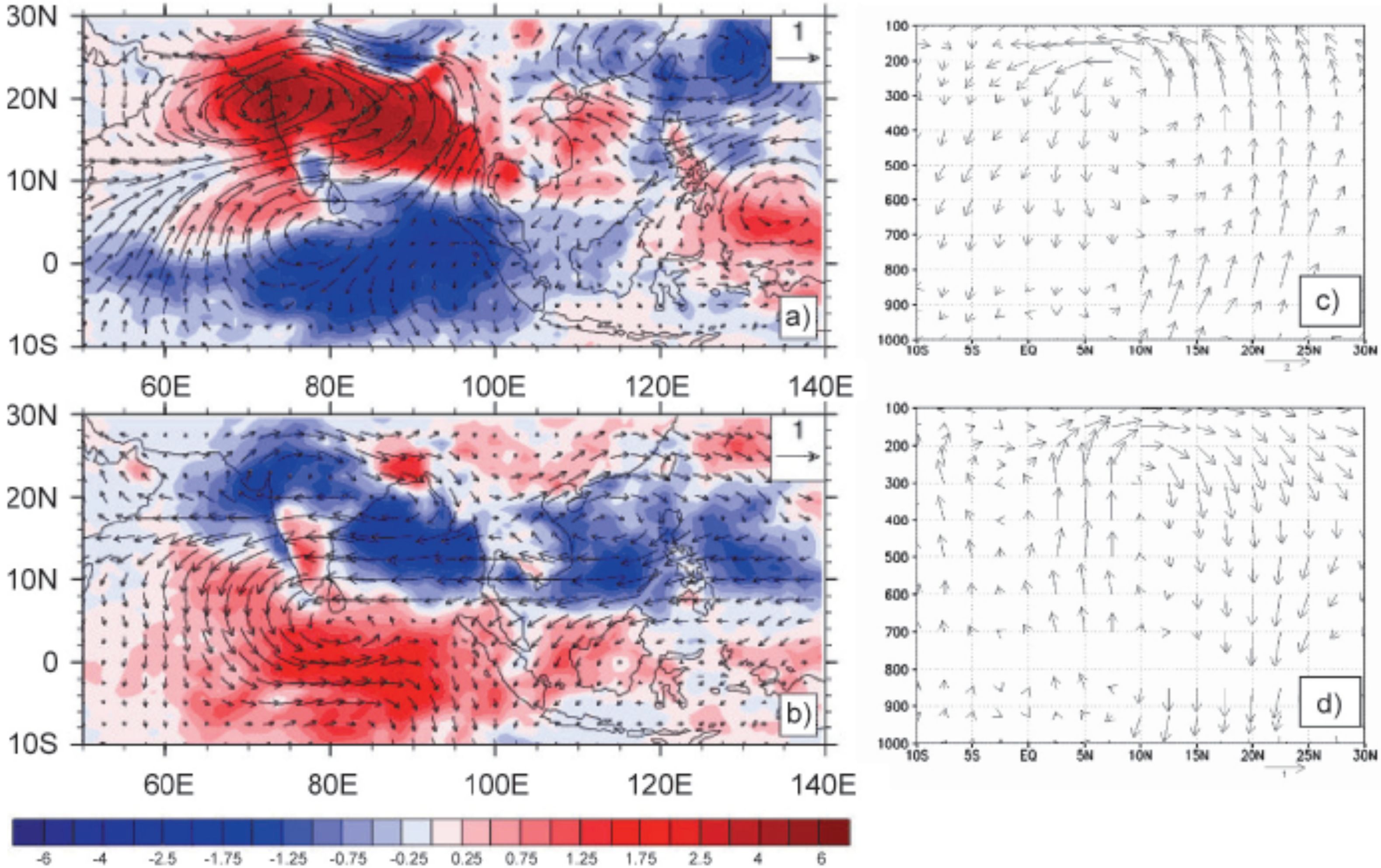

Figure 2.5. Horizontal and vertical structure of dominant ISV. Regressed 10 to 90-day filtered GPCP (shaded, mm day^{-1}) and zonal and meridional wind anomalies at 850 hPa (vectors, m s^{-1}) with respect to the ISO index (Figure 2.4) at (a) 0 lag (active condition) and (b) 14-day lag (break condition). (c) and (d) The anomalous regional Hadley circulation associated with active and break conditions, respectively. Regressed meridional and vertical wind anomalies at a number of vertical levels averaged over 75°E–85°E. Vertical wind anomalies (h Pa s^{-1}) have been scaled up by a factor of 100.

Goswami, 2011, ISV Book,Chapt-2

Convectively Coupled…

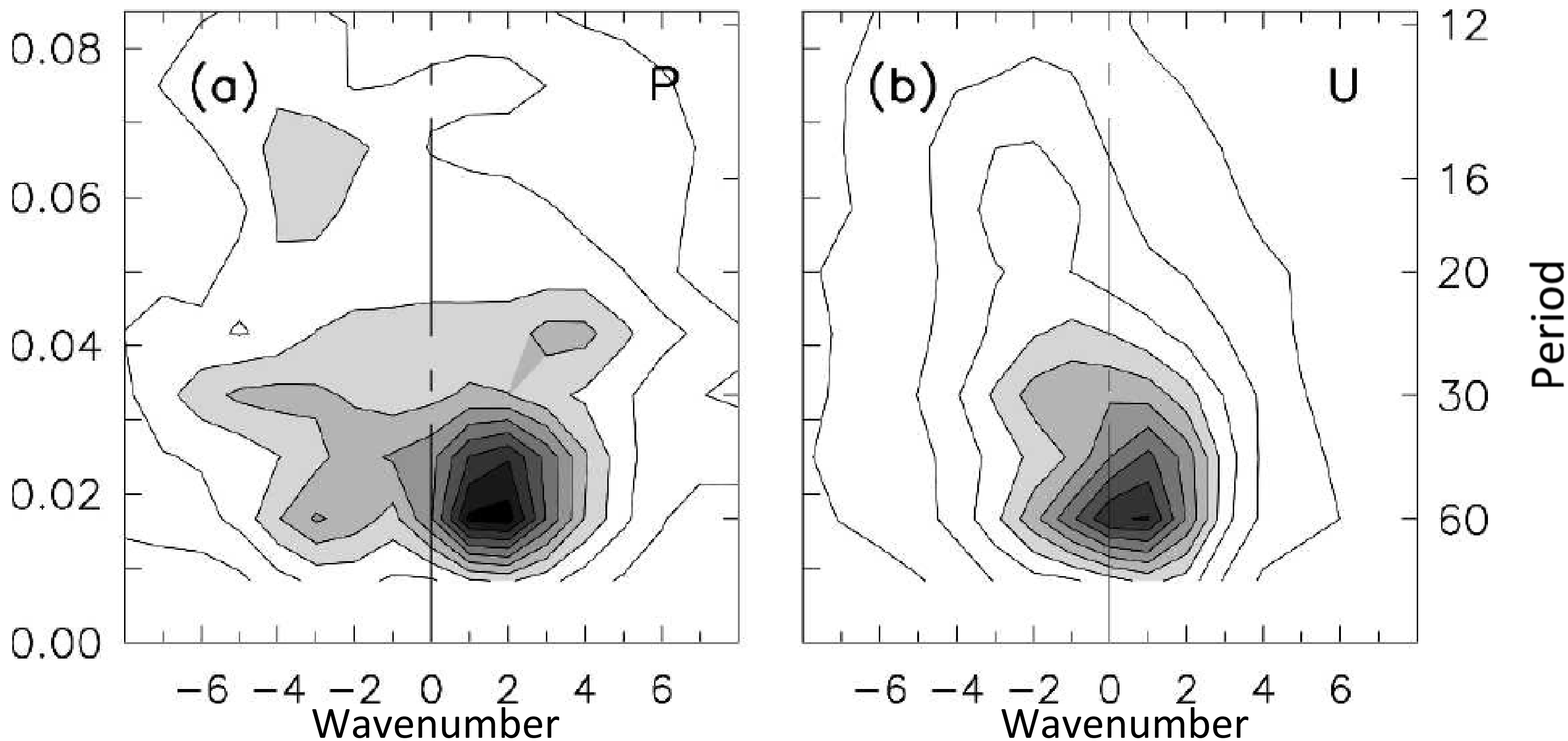

FIG. 2. Wavenumber–frequency spectral power of observed precipitation and 850-hPa zonal winds anomalies averaged over the latitude band 5°–25°N. The *y* axis left ordinate is frequency (in cycles per day, cpd) and right ordinate is period (days), while the *x* axis represents zonal wavenumber. The minimum contour and contour interval is 0.5; contours greater than 2.0 are shaded.

A new Index for real time monitoring and forecast verification of MISO

Suhas , Neena and Goswami , 2012, Climate Dynamics

Phase composite of Precipitation anomaly

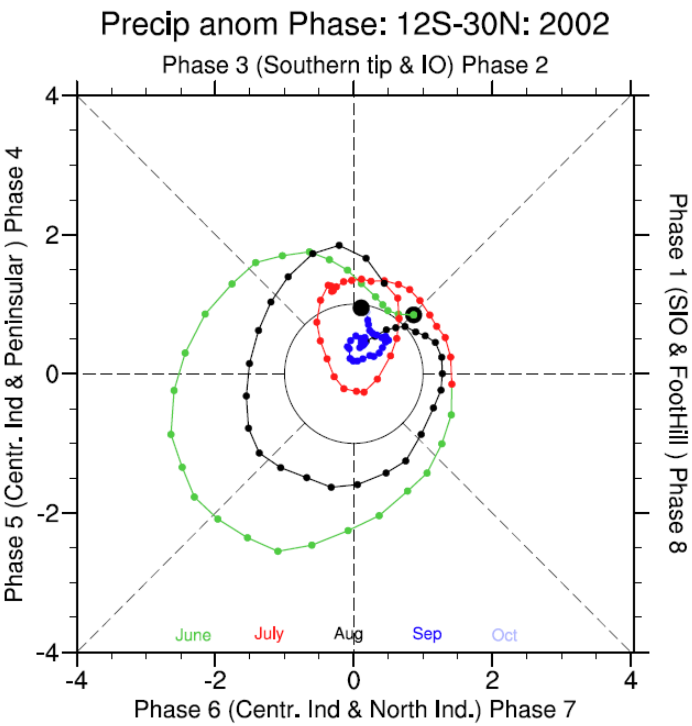

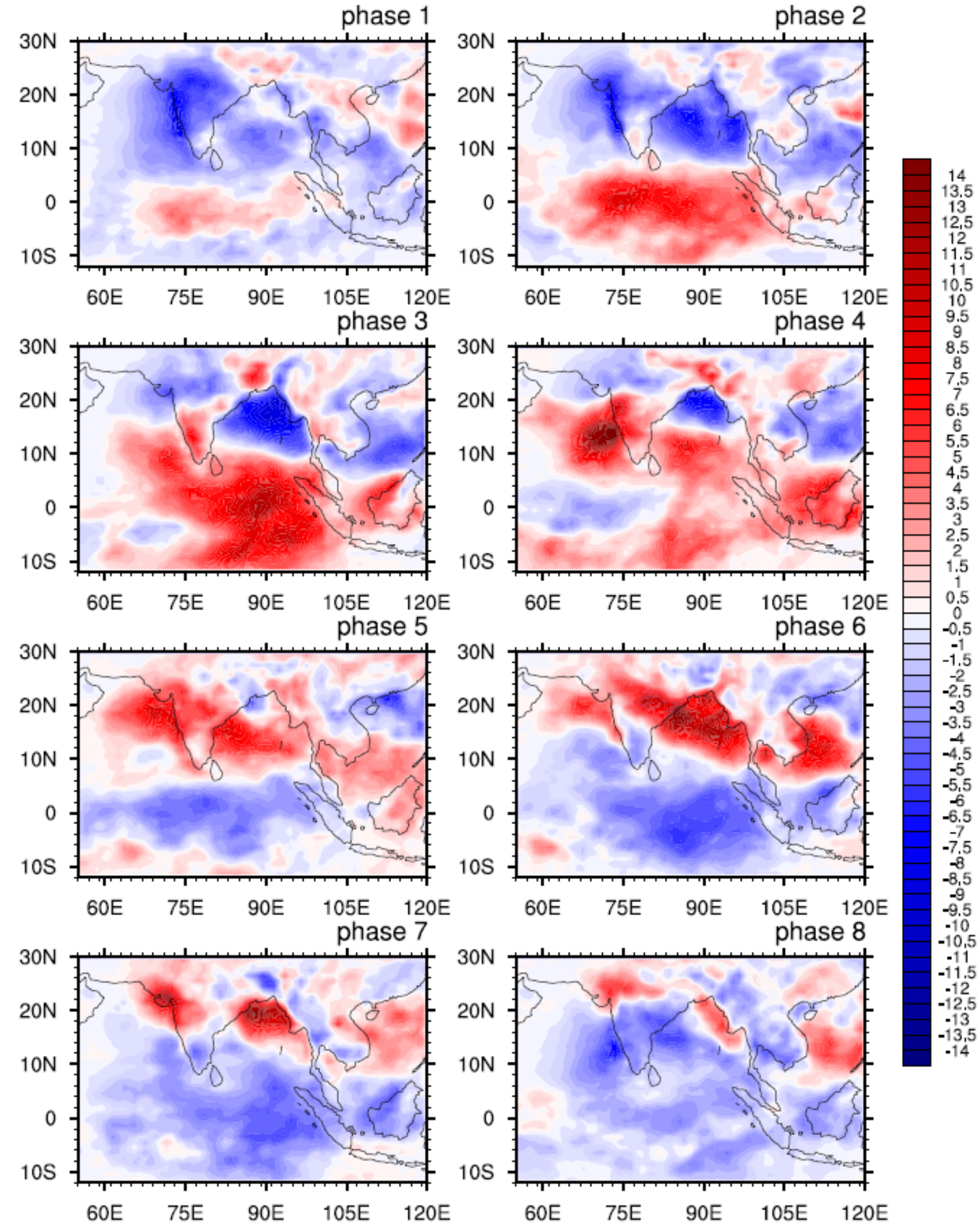

s.d. of 10-90 filtered GPCP daily rainfall

s.d. of Interannual variabiloty of seasonal mean rainfall

Amplitude of annual cycle of rainfall (JJA-DJF)

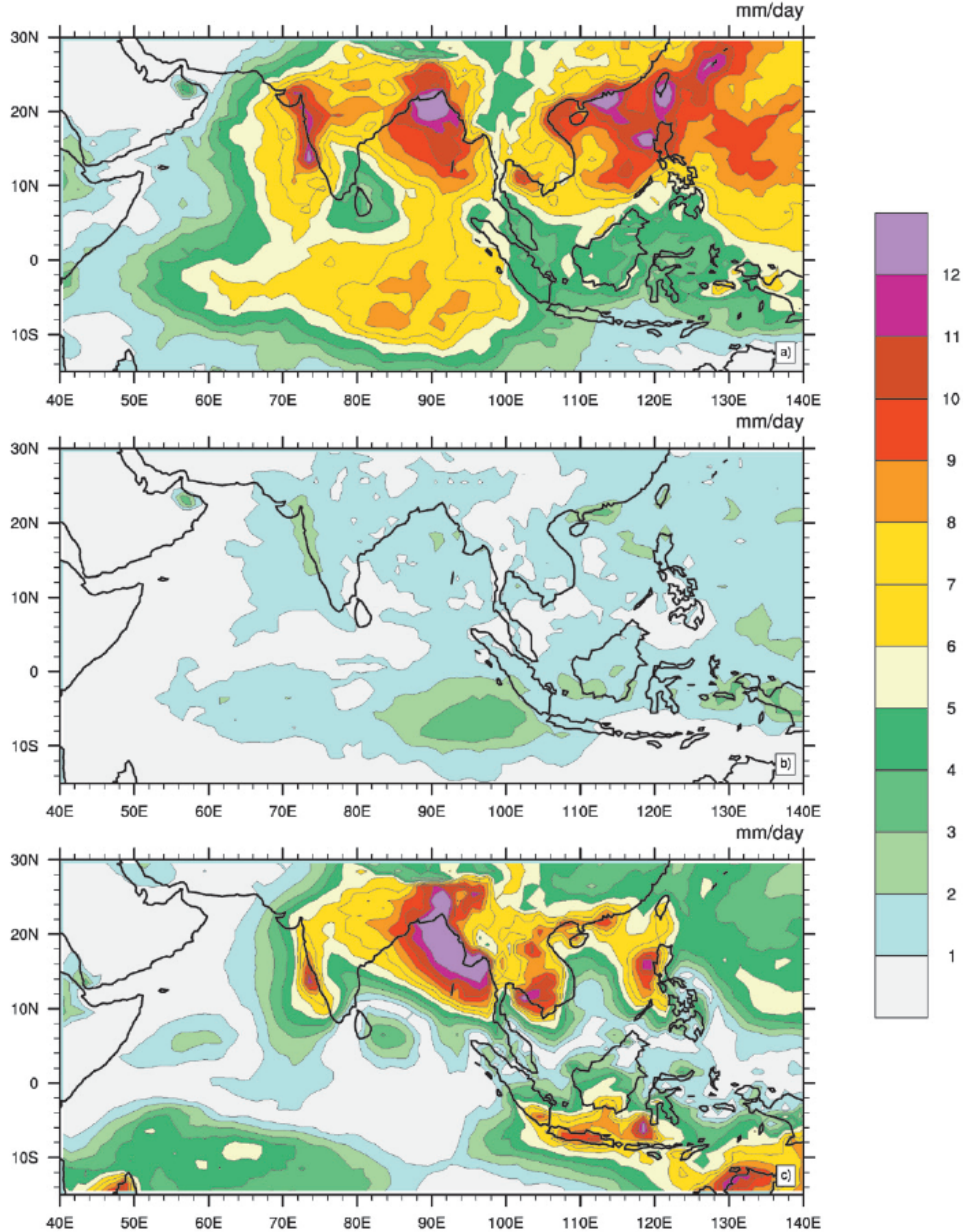

Figure 2.3. (a) Standard deviation of 10 to 90-day filtered GPCP precipitation anomalies (mm/day) based on 1997–2007 JJAS seasons. (b) Standard deviation of IAV of JJAS seasonal mean for the period 1997–2007. (c) Amplitude of the annual cycle. Climatological mean absolute value of the difference between JJAS mean and DJF mean for the 1997–2007 period from GPCP.

Why Indian monsoon ISV is important?

They represent a very large signal and hence potentially predictable!

ISOs Modulate Monsoon Synoptic Activity

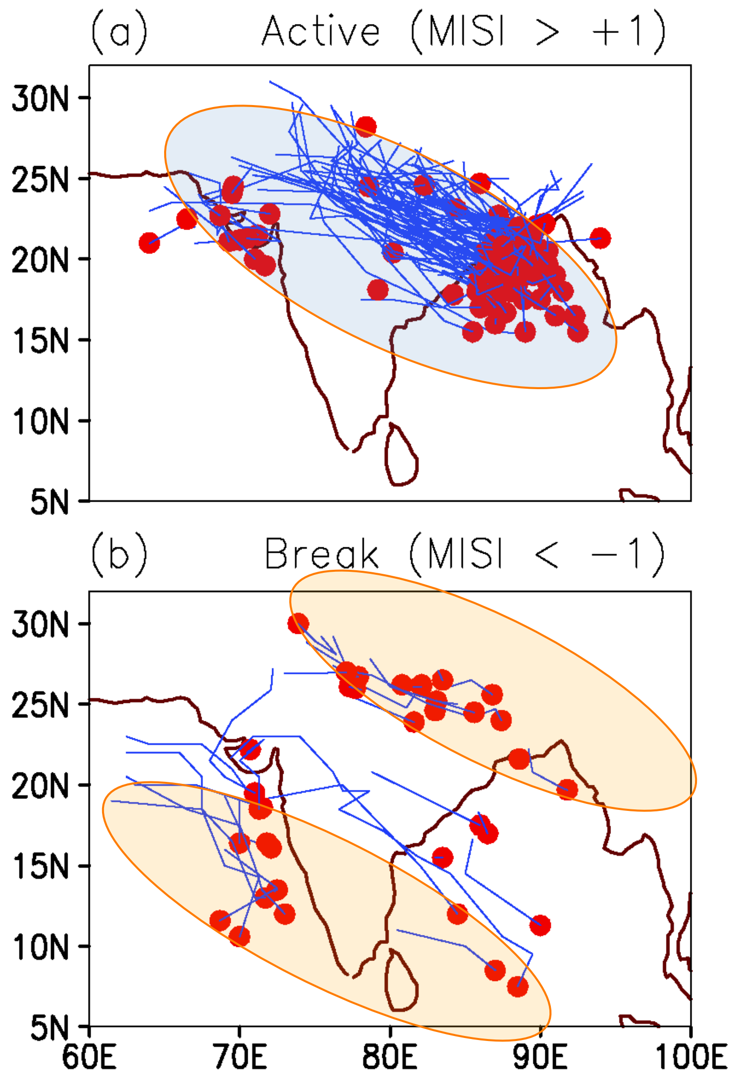

Tracks of LPS for the period 1954-1983 during extreme phases of monsoon ISO. (a) 'Active' ISO phase (MISI > +1) and (b) 'Break' ISO phase (MISI < -1). Red dots represent the genesis point and their lines show the tracks.

Goswami et al. 2003, *GRL*, 30, doi: 10.1029/2002GL016734

Scale Selection: What selects the 30-60 day time scale?

As the zonal scale of the 30-60 day mode (MISO) is very large compared to its meridional scale, Zonally symmetric General Circulation model (GCM) can be used to study its dynamics like a. ITCZ model

➔We used GLAS Symmetric Climate Model with radiative forcing and interactive convective parameterization

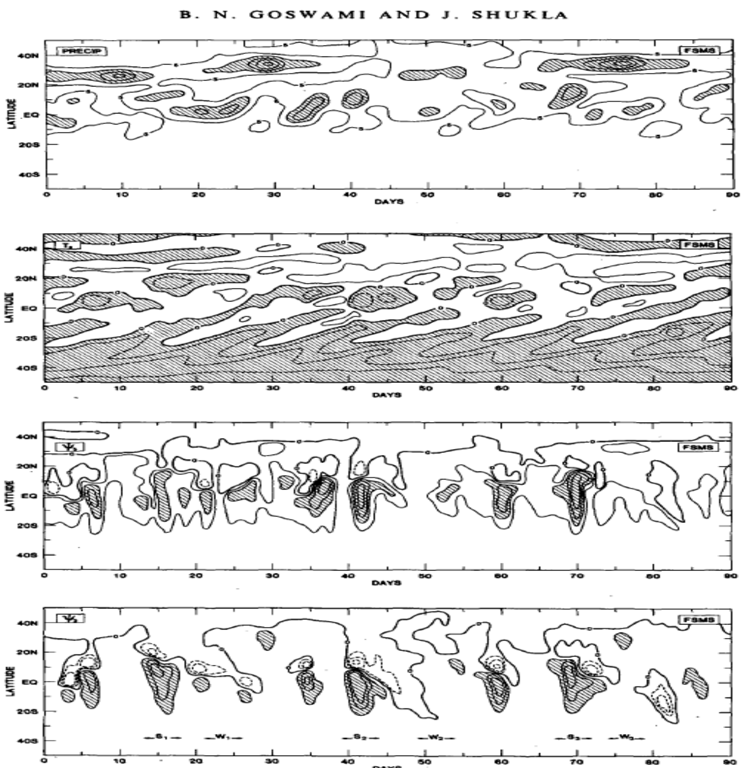

FIG. 4. As in Fig. 2 but for the fixed soil moisture, summer (FSMS) run. A unit of 300 is subtracted from the TS field and negative areas are shaded. Contour interval for TS and P is 10, and that for ψ_5 is 25. For ψ_2, negative contour interval is 10 and positive contour interval is 20. For P, contours greater than 15 are shaded, for ψ_5 contours greater than 50 are shaded while for ψ_2, contours greater than 20 are shaded.

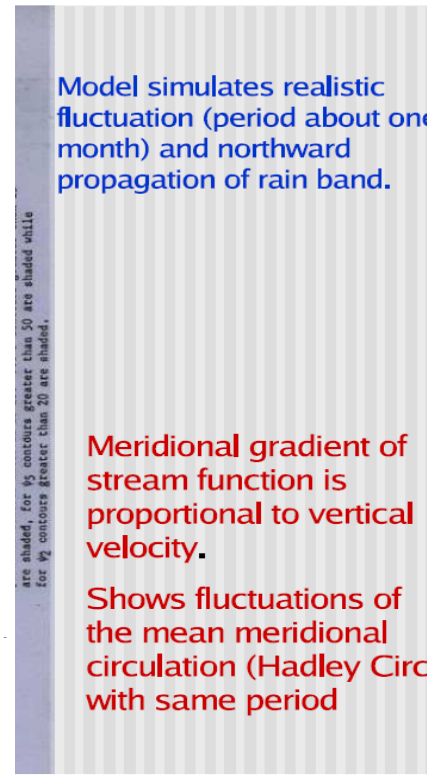

Model simulates realistic fluctuation (period about one month) and northward propagation of rain band.

Meridional gradient of stream function is proportional to vertical velocity.

Shows fluctuations of the mean meridional circulation (Hadley Circ with same period

Goswami and Shukla, 1984, JAS

Figure 10: Latitude-time plot of some simulated fields by the GLAS Symmetric climate model.

Scale Selection: What selects the 30-60 day time scale?

JOURNAL OF THE ATMOSPHERIC SCIENCES V

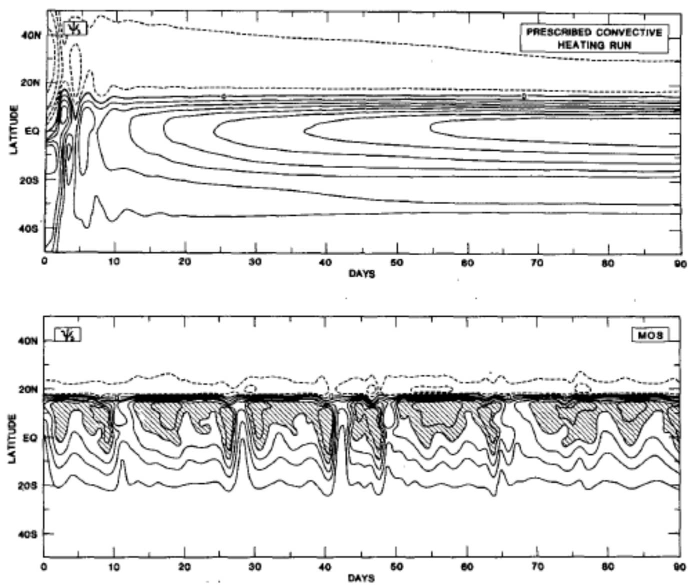

FIG. 3. Time series of ψ_5 for a run with prescribed latent heating (upper panel) and dynamically determined heating (lower panel) for the all-ocean summer run (MOS). Units 10^{10} kg s^{-1}.

When interaction of the convective heating with circulation is switched off by prescribing a heating and keeping it fixed with time,

The Oscillations of the Hadley circulation disappear!

Net Radiative effect warms up the surface making temperature profile unstable. Builds dry and moist instability.

Latent heat of convection heats atmosphere, CISK leads to intensification of the ITCZ

Intensification of ITCZ➔Heating upper atmosphere & Increased cloudiness➔ cooling of surface.

Temperature profile➔stable ➔ ITCZ weakens ➔ clear clouds ➔ solar radiation heats surafce

While the Radiative-convective –dynamical feedback leading to the MISO (30-60 day mode) is robust, more insight about the process has been unraveled by several simpler theoretical studies that followed; e.g.

Bin Wang and X. Xie, 1997: A Model for the Boreal Summer Intraseasonal Oscillation, J. Atmos. Scie., 54, 72-86, https://doi.org/10.1175/1520-0469(1997)054<0072:AMFTBS>2.0.CO;2

More recently, both the MJO and the MISO are being looked at as natural modes of the 'moist tropical atmosphere' known as 'moisture modes' that do not exist in dry atmosphere. e.g.

S. Wang and Adam Sobel, 2022: A Unified Moisture Mode Theory for the Madden–Julian Oscillation and the Boreal Summer Intraseasonal Oscillation, J. Climate, 35, 1267-1291

Northward Propagation of the MISO

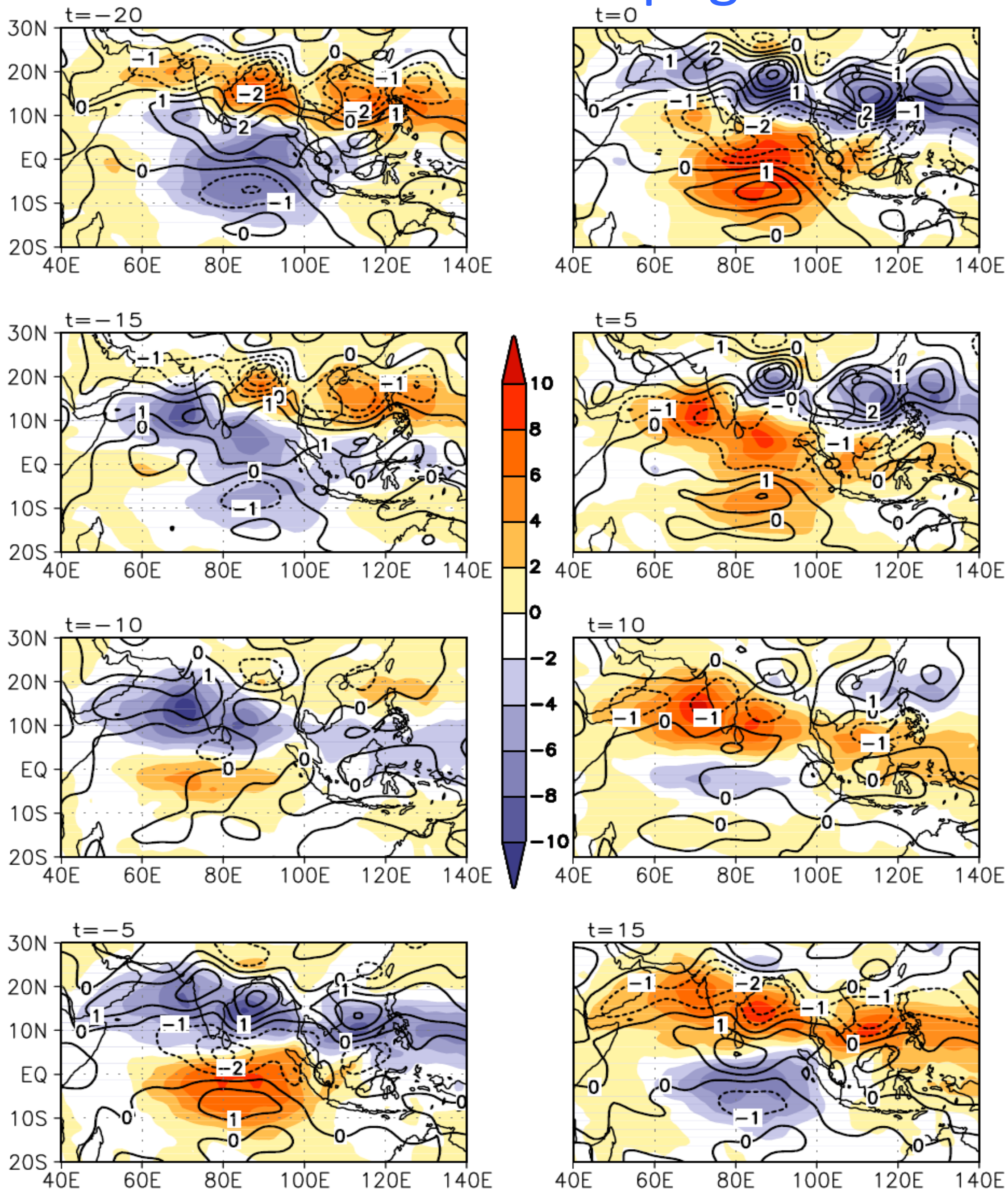

Large scale structure: relationship between OLR and 850 hPa vorticity

Regressed OLR (shaded) and 850 hPa relative vorticity (contour) w.r.t a reference time series of 10-90 day filtered OLR over CI

Goswami, 2005: ISV book Lau & Waliser (Eds)

Northward Propagation of the MISO

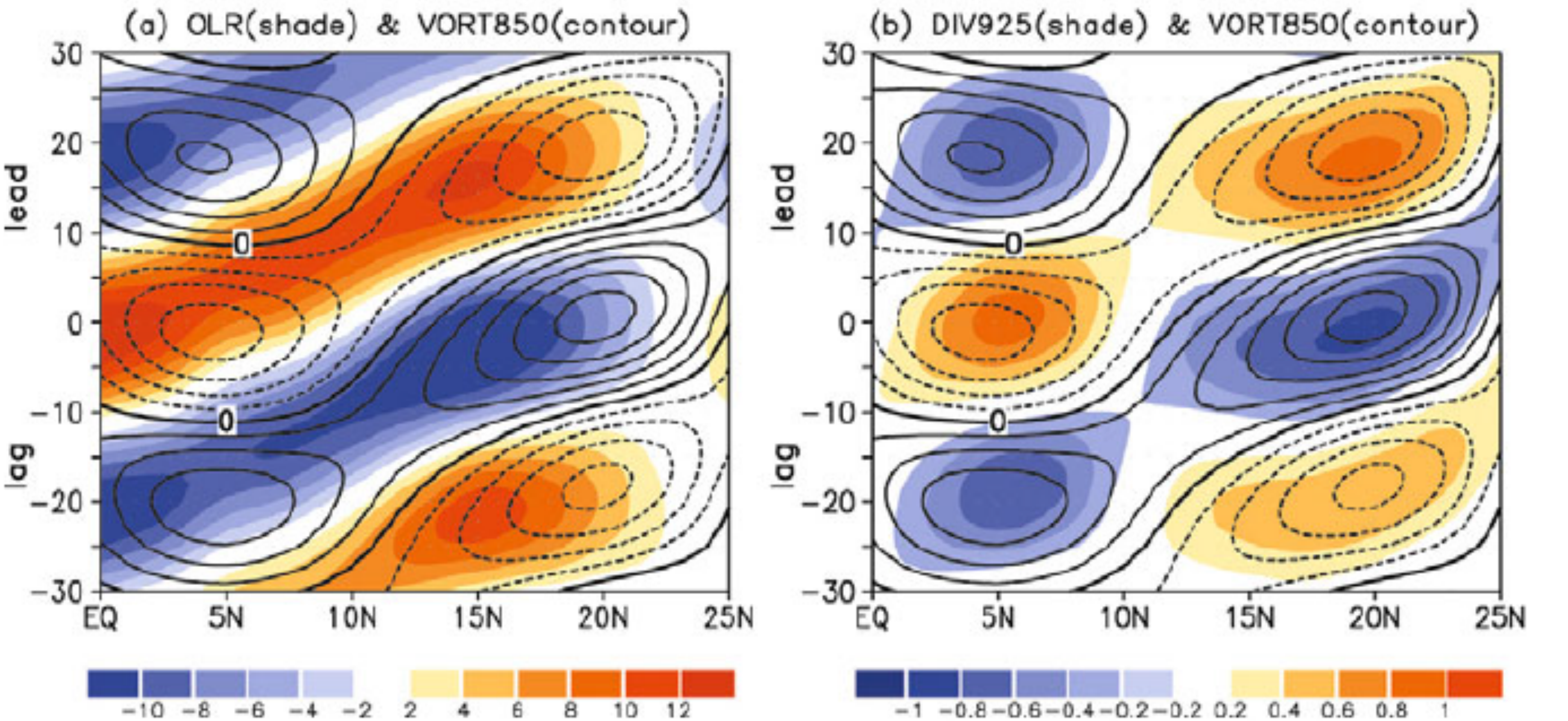

Figure 2.16. (a) Regressed 30 to 60-day filtered anomalies of OLR (shaded; W m^{-2}) and 850 hPa relative vorticity (contour, positive solid and negative dashed, contour interval 1×10^{-6} s^{-1}) with respect to the reference time series described in Figure 2.10 averaged over 80°E–90°E. (b) Regressed 30 to 60-day filtered anomalies of 850 hPa relative vorticity (contour, positive solid and negative dashed, contour interval 1×10^{-6} s^{-1}) and divergence at 925 hPa (shaded; 10^{-6} s^{-1}) with respect to the same reference time series.

Goswami 2011. ISV book (Lau and Waliser)

Mechanism of Northward Propagation of Monsoon ISO's

Two Possible mechanisms

1. Northward shift of boundary layer moisture convergence through advection by ISO winds in the presence of northward gradient of mean moisture in the low levels

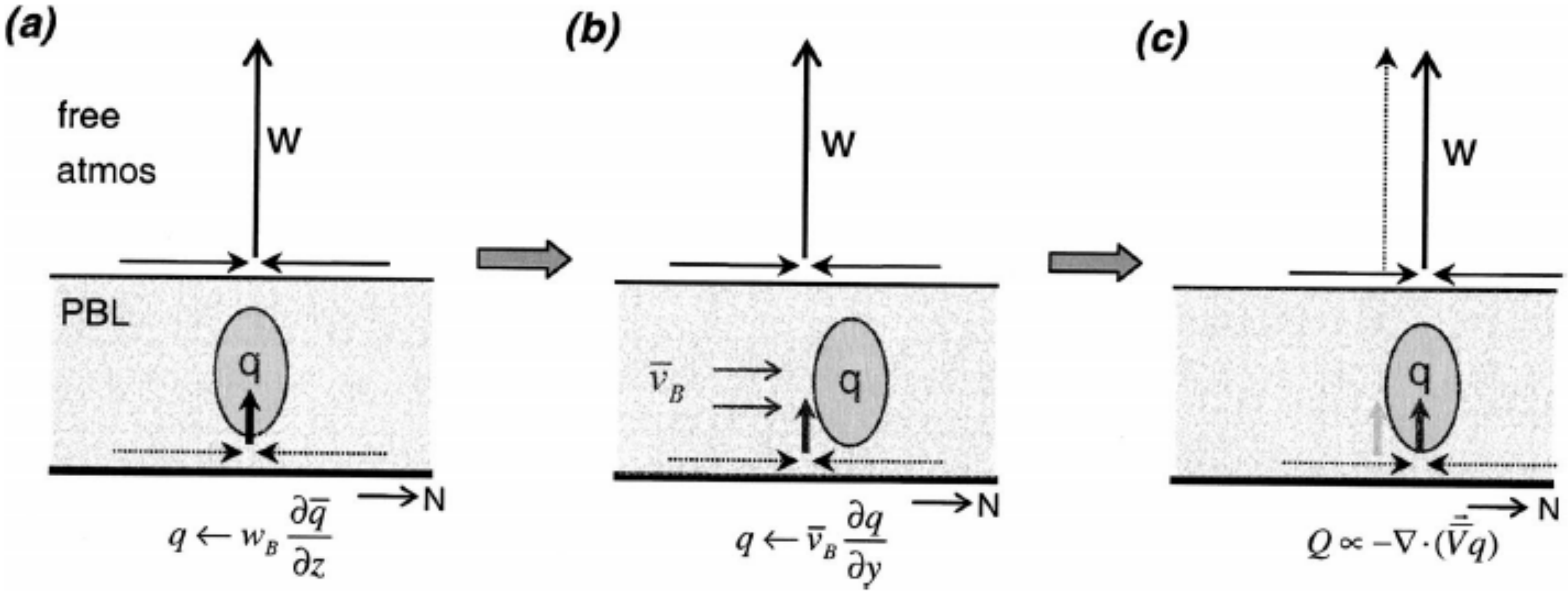

FIG. 12. Schematic diagram for the mechanism of moisture advection by mean flow. (a) The specific humidity perturbation caused by Ekman pumping is advected (b) by the mean northward meridional wind in the PBL, (c) which leads to the northward shift of moisture convergence and thus convective heating to the convection center.

Jiang et al., 2004: J. Climate, Vol. 17, 1022-1039

Mechanism of Northward Propagation of Monsoon ISO's

Two Possible mechanisms

2. Northward shift of boundary layer moisture convergence as a response of baroclinic heat source in the presence of background of Easterly shear of mean winds

1 March 2004 JIANG ET AL. 1033

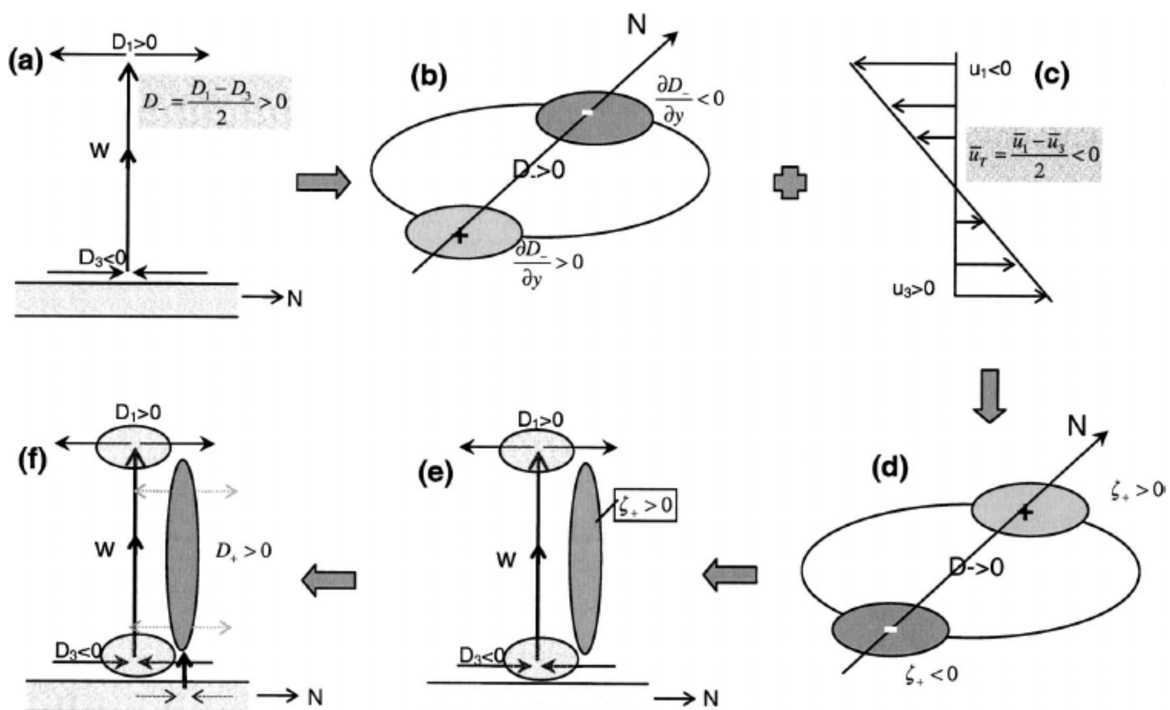

FIG. 10. Schematic diagram for the vertical shear mechanism. (a) Consider initially an ISO convection with a baroclinic structure. (b) This leads $\partial D_-/\partial y < 0$ ($\partial D_-/\partial y > 0$) north (south) of the convection center. (c) In the presence of the easterly shear of the mean flow, (d), (e) a positive barotropic vorticity is induced north of the convection, leading to (f) a barotropic divergence in situ. The latter further leads to a PBL convergence and thus a northward shift of convective heating.

Potential Predictability of monsoon ISOs

- **Existence of a large 'signal' (amplitude of ISO's) is the basis for potential predictability of Monsoon ISO's**

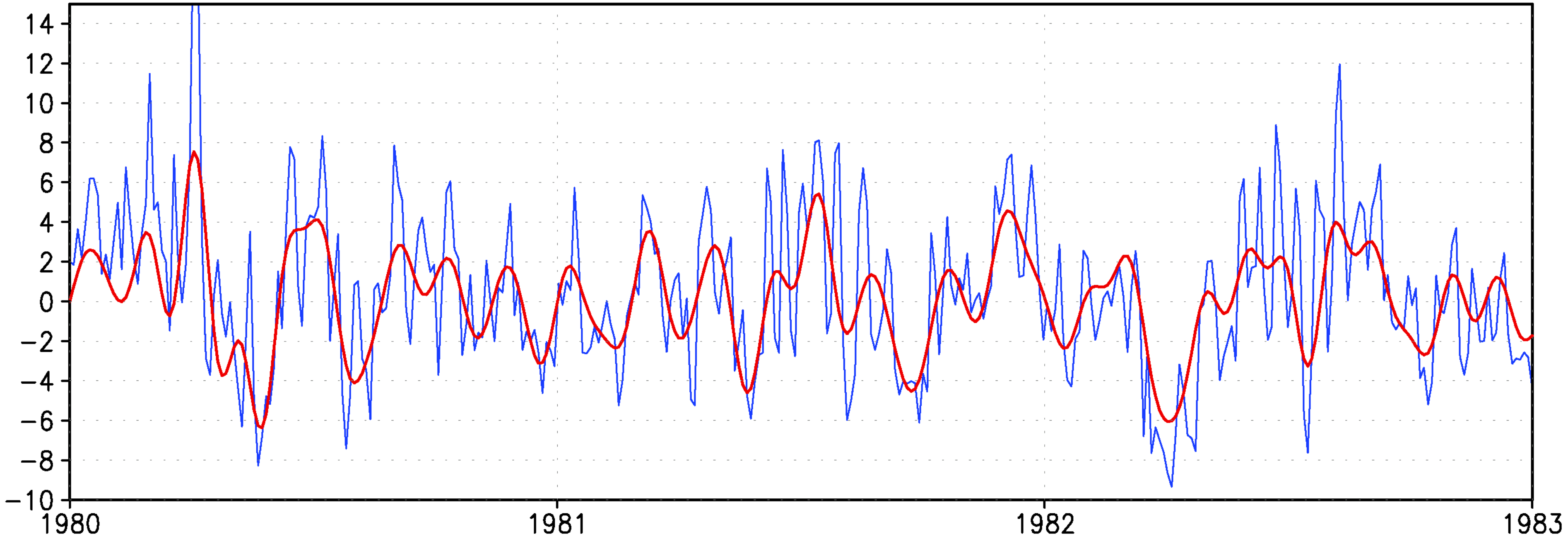

Time series of daily rainfall anomaly (mm/day) over central India (blue) during 1 June – 30 Sept. for three years and 10-90 day filtered (red) rainfall.

What is the limit on the Indian monsoon ISO predictability?

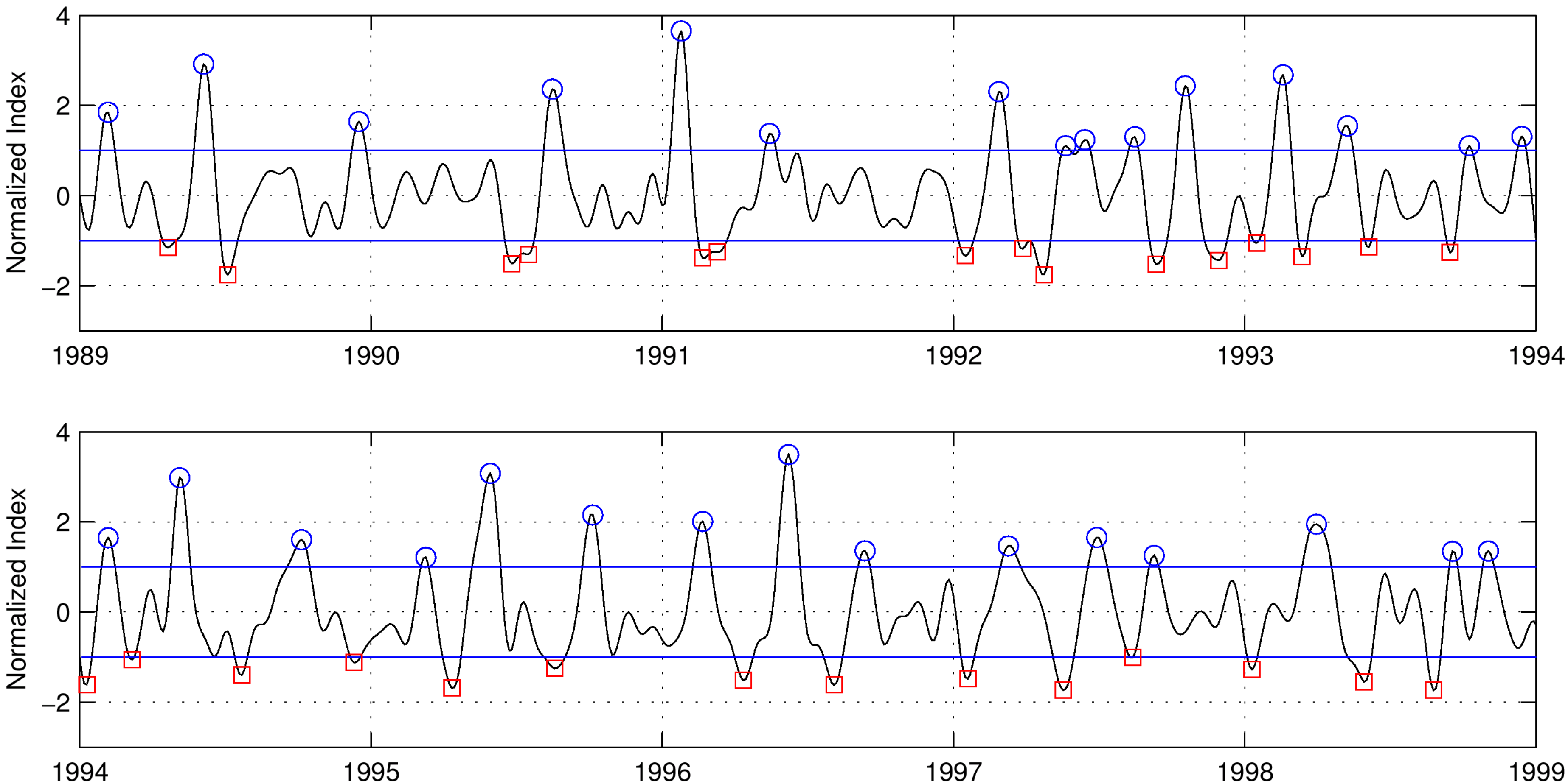

10-90 day filtered precipitation (CMAP) averaged over Box I normalized by its own standard deviation shown here for 10 summers (1 June- 30 Sept.). Blue circles → peak wet spells (active conditions); red squares → peak dry spells (break in monsoon).

Gosewami and Xavier, 2003, GRL

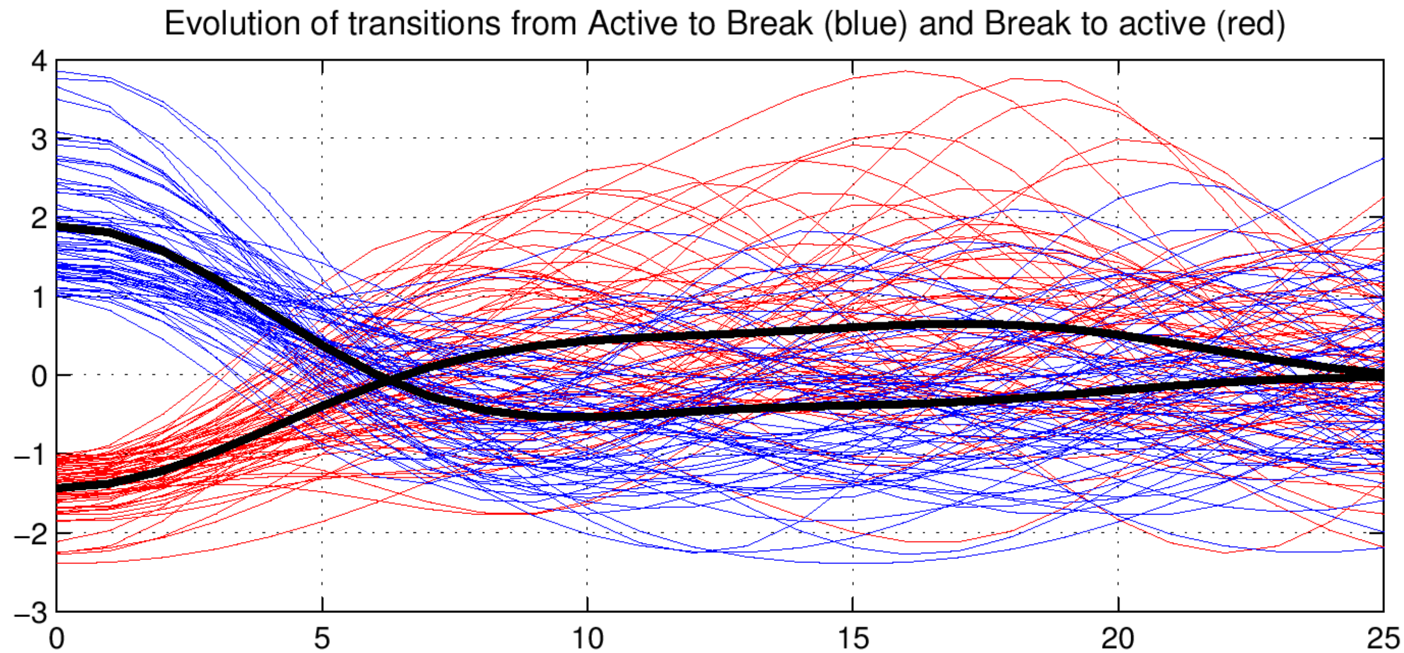
Evolution of transitions from Active to Break (blue) and Break to active (red)

CMAP

Box-I

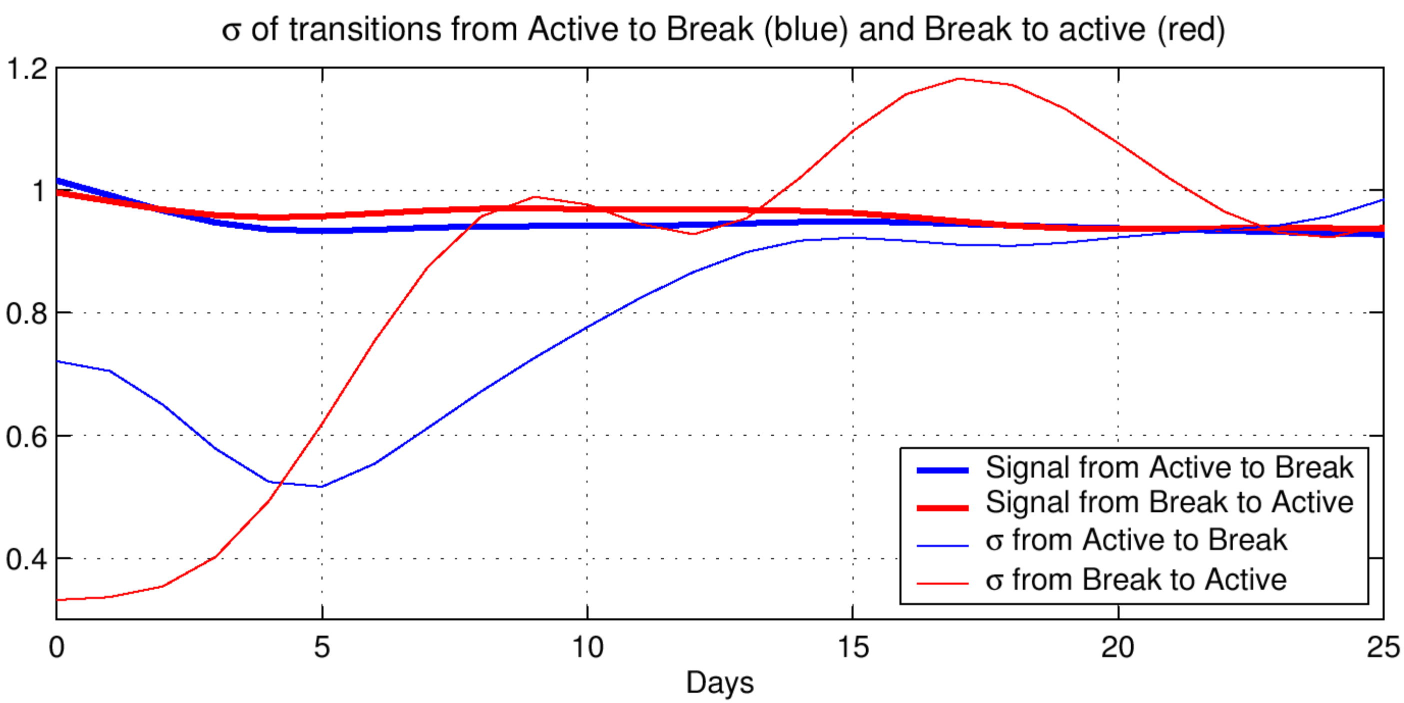
σ of transitions from Active to Break (blue) and Break to active (red)
Days
Signal from Active to Break
Signal from Break to Active
σ from Active to Break
σ from Break to Active

Sub-Seasonal variations of Indian monsoon interaction with Seasonal mean ISMR

Climate or the time mean is aggregate of **Weather** or sub-seasonal fluctuations

It is natural to expect that the statistics (periodicity, variance etc) of sub-seasonal fluctuations are related to the seasonal mean monsoon.

Long 'breaks' ➔ 'poor' monsoon

'Strong' monsoon➔ no long breaks

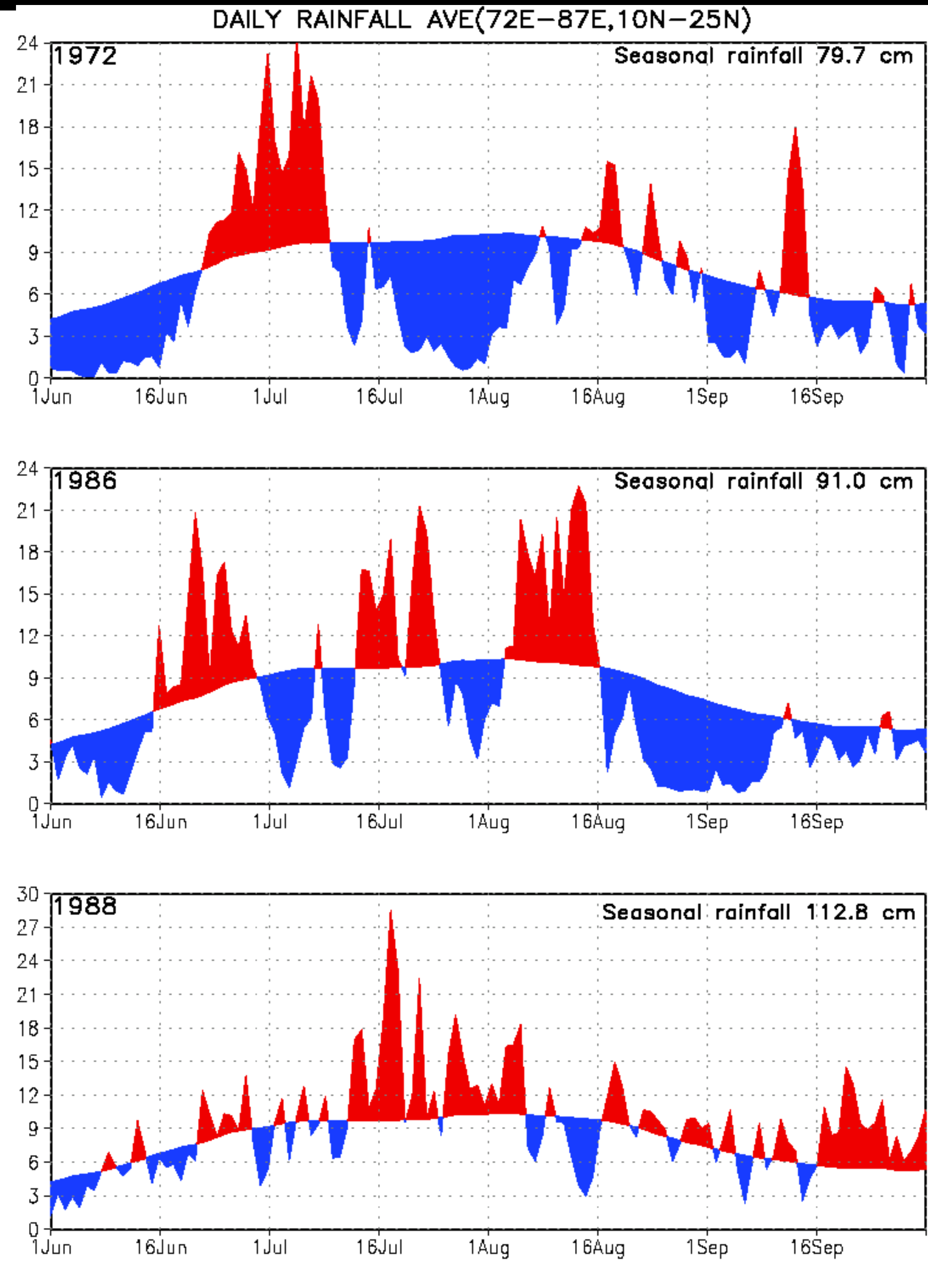

Sub-Seasonal variations of Indian monsoon interaction with Seasonal mean ISMR

Using daily OLR data between 1975 and 1997 (22-years), Laewrence and Webster (2001) show that,

➔Variance of ISO filtered OLR anomaly (25-80 day filtered) correlate *positively* with the anomaly of seasonal mean OLR (Fig)

➔The amplitude of ISO is *inversely* related to seasonal mean rainfall anomaly

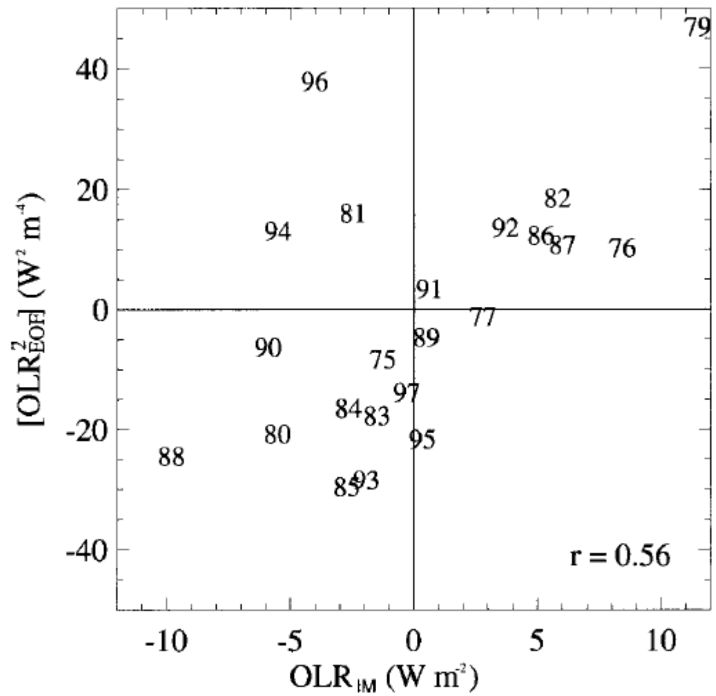

FIG. 8. Scatter diagram of $[OLR^2_{EOF}]$ vs OLR_{IM}. Both indices are plotted as anomalies from their respective 22-yr means. The correlation is 0.56.

TABLE 3. Correlations between seasonal ISO activity index ($[OLR^2_{EOF}]$) and south Asian monsoon indices over 22 yr (1975–97, excluding 1978). A correlation coefficient greater than ±0.36 is statistically significant at 95% confidence level.

Monsoon index	JJAS ISO activity $[OLR^2_{EOF}]$
AIRI	−0.45
OLR_{SAM}	0.30
OLR_{IM}	0.56
OLR_{BB}	0.17

Lawrence and Webster, 2001: J.Climate

https://doi.org/10.1175/1520-0442(2001)014<2910:IVOTIO>2.0.CO;2

31-year moving correlation between variance of synoptic (red), QBM (green) and MISO (blue) during JJAS and anomaly of seasonal mean ISMR using Rajeevan et al.,(2008) data between 1901 and 2014

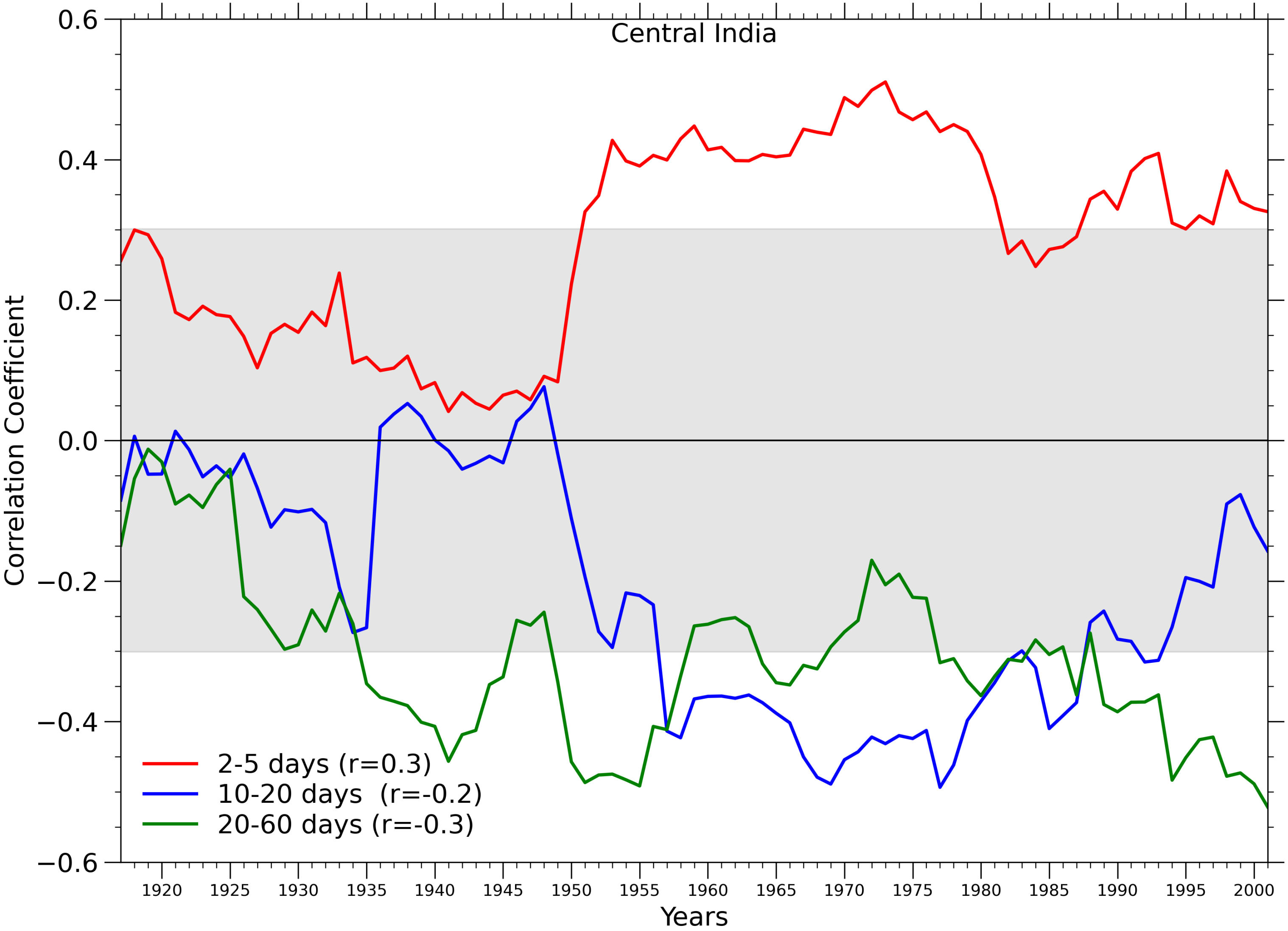

Courtesy,
Prolay Saha

How can we understand the positive contribution of synoptic variance to the seasonal mean?

Let's start with External forcing like La Nina that starts with a stronger ΔTT trying to strengthen the monsoon circulation.

Monsoon starts with stronger low level cyclonic vorticity at 850 hPa → stronger N-S horizontal zonal wind shear around monsoon trough

Synoptic disturbances being instabilities of background mean flow, → frequent and stronger lows & depressions → more rain

More rainfall leads to further strengthening the 'external' background ΔTT → stronger monsoon

+ve feedback

- While the correlation between variances of synoptic disturbances and seasonal mean could be understood, the same is not true for the correlations between variances of QBM and MISO with the seasonal mean.

- As found by Lawrence and Webster (2001), we find the variances of both the QBM and MISO correlate inversely with the seasonal mean. The physical mechanism of how this happens is not yet quite clear.

Thank you

As asked during the last Lecture, time series of Dipole Mode Index (DMI) can be found and downloaded from NOAA website through the following link,

https://psl.noaa.gov/gcos_wgsp/Timeseries/DMI/

Chen and Chen 1993

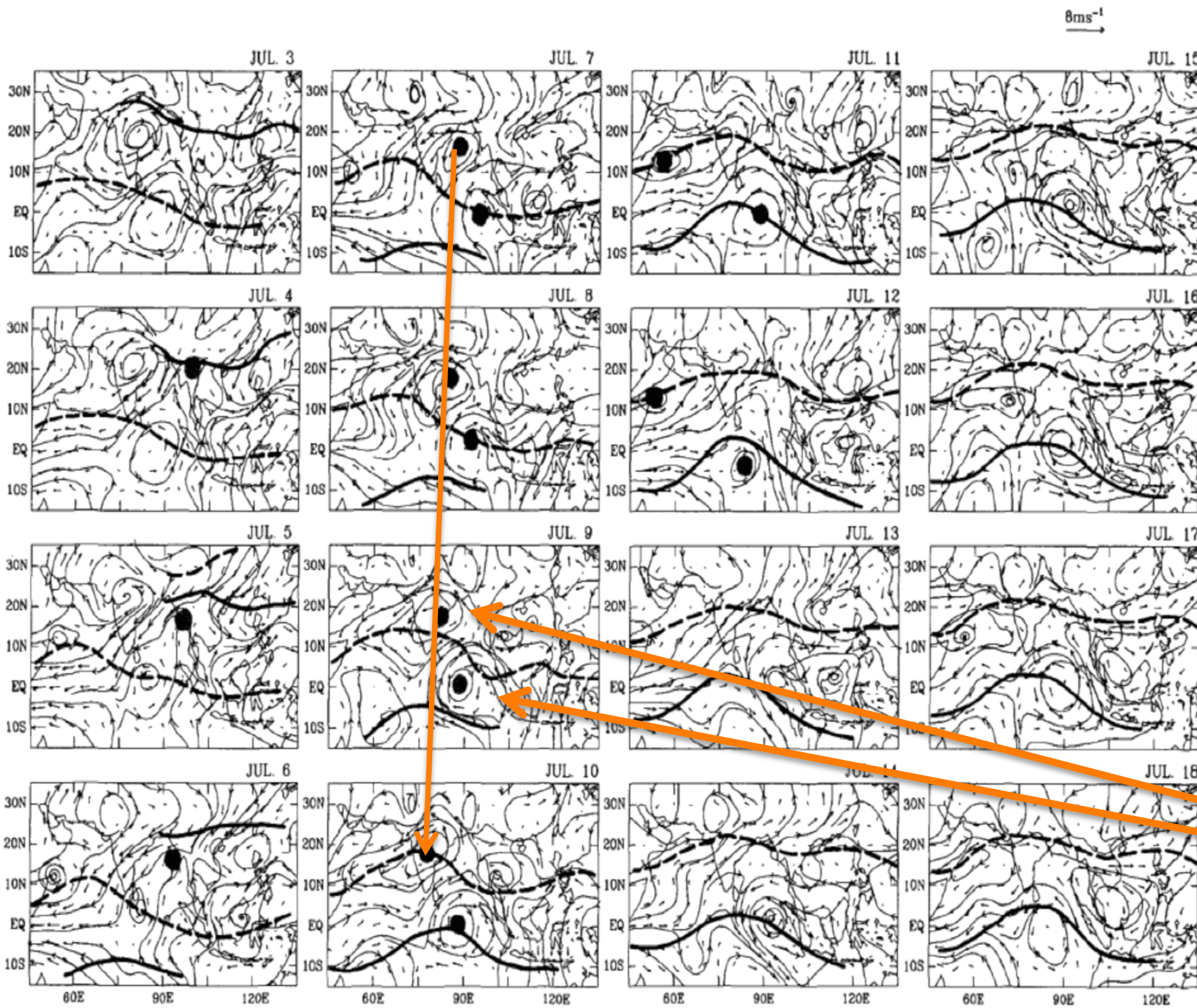

FIG. 7. Streamline synoptic charts constructed with the 10–20-day filtered 850-mb wind $\tilde{V}$(850 mb) for the first major monsoon rainfall spell after the 1979 Indian monsoon onset. The 30–60-day transient monsoon troughs (thick solid lines) and ridges (thick dashed lines) are superimposed on these synoptic charts. The low centers of the 10–20-day monsoon mode are stippled.

Twin Cyclonic vortices centered around 10N.
Equatorial Rossby wave?

QBM in winter : Kiladis and Wheeler 1995, JGR

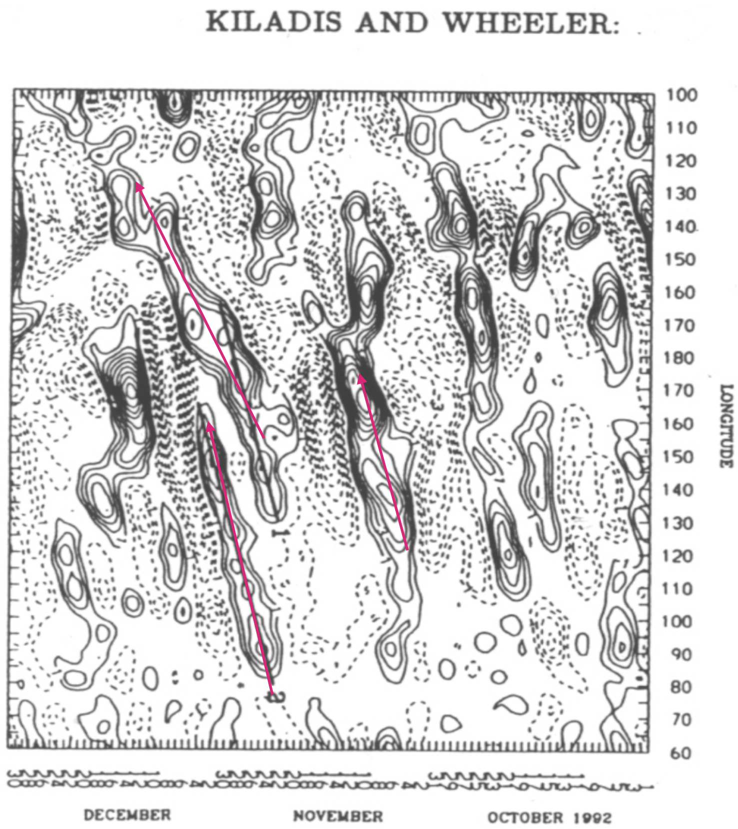

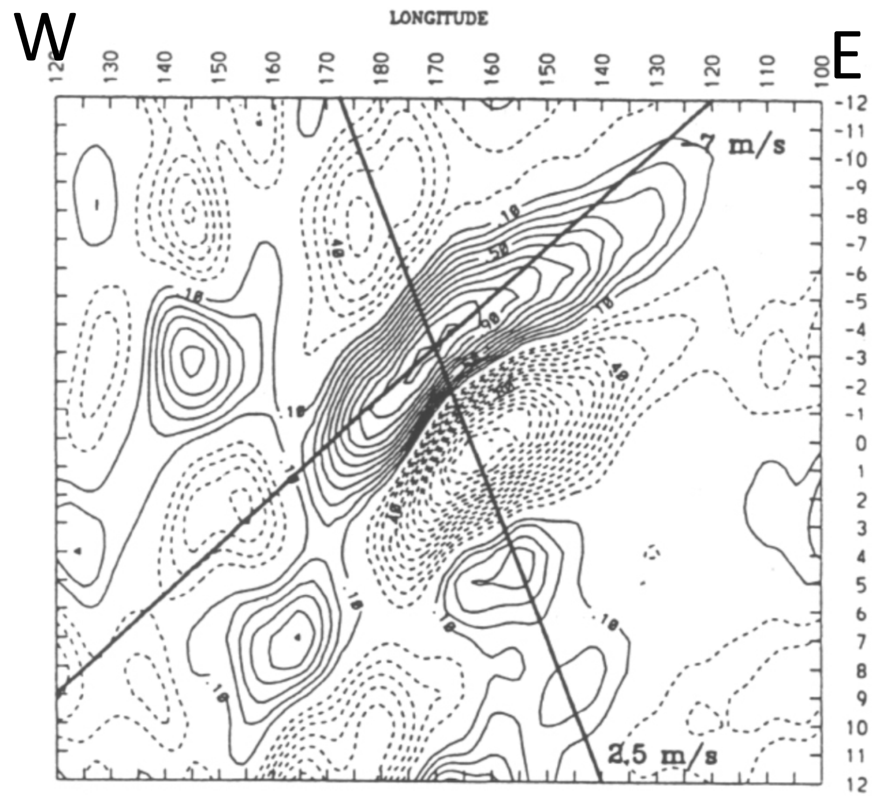

6-30 day filtered 850 hPa zonal wind anomaly along the equator , Oct 1- Dec 31,1992, TOGA COARE IOP

Phase composite of the ER wave based on 8 year daily analysis. T~12 days, λ~6000km, Cp~ -7m/s but less than -5 m/s in the western Pacific, Cg~+2.5 m/s

Role of the mean background flow on the unstable mode:

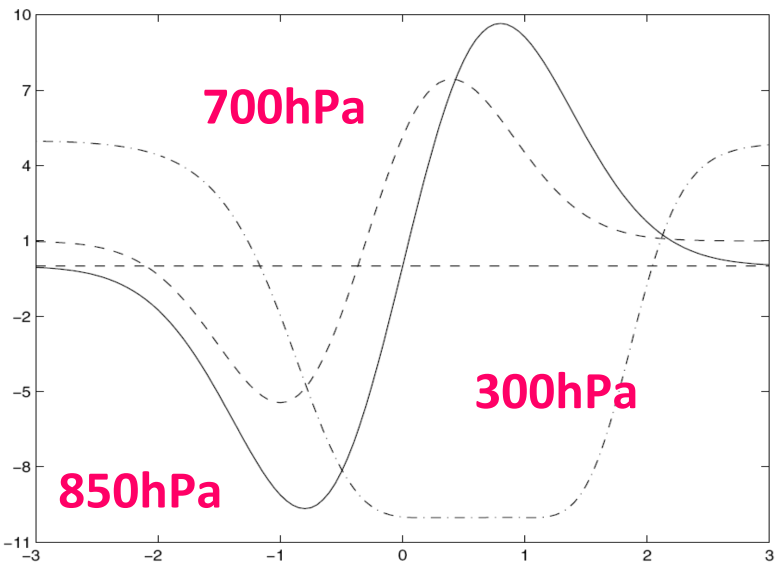

Climatological zonal winds for July averaged between 40E-120E

T=17 days, λ = 6020 km

Cp = 4.1 m/s

Spatial structure of the unstable mode with mean flow.

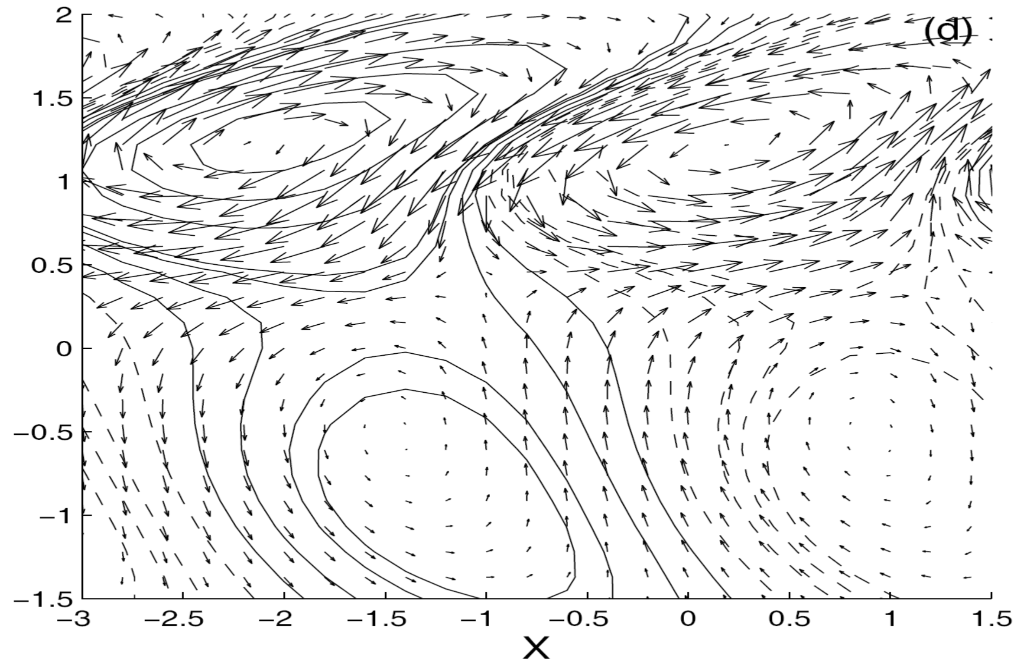

Vertical shear of mean winds:

Not essential for the basic instability. When included makes the structure more realistic.

Evaporation wind feedback:

Again not essential for the basic instability. When included enhances the growth rate of the unstable mode without changing the period and phase speed substantially.

Importance of QBM in Tropical Intraseasonal Variability